Report Number: WI/SPR-04-97

PB2001-103540

INVESTIGATION OF MODIFIED APSHALT

PERFORMANCE USING SHRP BINDER SPECIFICATION

Final Report

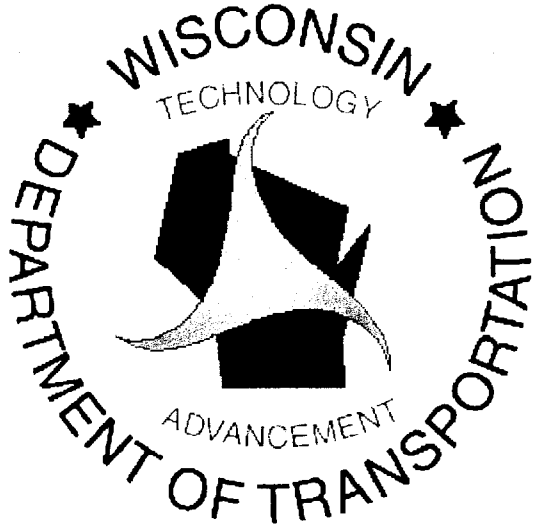

August 1997

INVESTIGATION OF MODIFIED ASPHALT PERFORMANCE USING SHRP BINDER SPECIFICATION WI/SPR-04-97

Final Report
Final Report Number: WI/SPR-04-97
WisDOT Highway Research Study #94-04
SPR #0092-45-73

Hussain U. Bahia, Ph.D.
Assistant Professor
Peter J. Bosscher, Ph.D., P.E.
Associate Professor

Jeffrey S. Russell, Ph.D., P.E.
Associate Professor

Suwitho Thomas
Research Assistant
Department of Civil and Environmental Engineering
University of Wisconsin - Madison
2210 Engineering Hall, 1415 Engr. Dr.
Madison, WI 53706

August, 1997

For

WISCONSIN DEPARTMENT OF TRANSPORTATION
Division of Transportation Infrastructure Development
Bureau of Highway Construction
Pavements Section
3502 Kinsman Boulevard, Madison, WI 53704

1. Report No. WI/SPR –04-97	2. Government Accessories No.	3. Recipient's Catalog No.
4. Title and Subtitle Investigation of Modified Asphalt Performance Using SHRP Binder Specification		5. Report Date August, 1997
6. Author(s) Hussain U. Bahia, Ph. D, Assistant Professor Peter J. Bosscher, Ph.D., P.E., Associate Professor Jeffrey S. Russell, Ph.D., P.E., Associate Professor Suwitho Thomas		7. Performing Organization Code
8. Performing Organization Name and Address University of Wisconsin – Madison Department of Civil and Environmental Engineering 2210 Engineering Hall, 1415 Engr. Dr. Madison, WI 53706		9. Performing Organization Report No. Report # WI/SPR – 04 – 97
		Work Units NO. (TRAIS)
11. Sponsoring Agency Name and Address Wisconsin DOT, Pavements Section 3502 Kinsman Blvd. Madison, WI 53704-2507		12. Contract or Grant No. ID-0092-45-73
		13. Type of Report and Period Covered Final – 12/94 to 7/97
14. Supplementary Notes		15. Sponsoring Agency Code WisDOT Study #94-04

16. Abstract:

The Pavement Research Division of the Wisconsin Department of Transportation (WisDOT) initiated this project as a result of concerns regarding excessive premature cracking of asphaltic pavements. The objectives of the project were to filed validate the Superpave binder specification criteria and to field validate the pavement temperature estimation procedure used in the original Superpave software.

Six test sections were constructed on USH 53 in Trempealeau County to monitor how weather conditions can affect pavement temperature at surface and as a function of pavement depth, using pavement instrumentation and a weather station. The asphalt cement used in the surface layer and the binder layer were varied for each test sections, and the type of mixture and pavement structure were similar for the six test sections. Two modified asphalts, graded at PG 58-34 and PG 58-40, and one conventional asphalt graded as PG 58-28 (120-150 penetration grade), were used in the study to investigate relation between thermal cracking and performance related properties of these asphalt binders.

This report includes analysis of the data collected during the first 22 months of the project. The analysis resulted in developing statistical models for estimation of pavement minimum and maximum temperature from meteorological data. The models (called the Wisconsin models) were compared to the Superpave recommended model and to the more recent model recommended by LTPP program. The analysis indicates that there is a strong agreement between the Wisconsin model and the new LTPP model for the estimation of minimum pavement design temperature. The analysis, however, indicates that the LTPP model and the Superpave model underestimate the maximum pavement design temperature at air temperatures higher than 40 °C. The analyses also indicate that there are significant differences between the standard deviation of air temperatures and the standard deviation of the pavement temperatures. The Wisconsin models and the pavement standard deviations are recommended for estimating the required PG grades to be used in Wisconsin.

The report also includes the results of the surface condition surveys and its relation to the properties of the asphalts used in the test sections. The performance analysis could not be used for evaluating the Superpave binder criteria because all sections suffered from reflective cracking. Although there were significant differences in severity of reflective cracking, no strong correlations could be found with asphalt binder properties. The results indicate that the modified binders used in this study did not result in reduction of reflective cracking.

17. Key Words

Pavement Temperature, Weather Data, Modified Asphalts, Superpave, Reflective Cracking

18. Security Classif. (of this report) Unclassified		19. Distribution Statement No restrictions	
	20. Security Classif. (of this page) Unclassified	21. No. of Pages 80	22. Price

ACKNOWLEDGMENTS

This research study was sponsored by the Wisconsin Department of Transportation. The work presented here would not have been possible without the cooperation and assistance of a great many individuals. Mr. Robert Schmieldlin and Mr. Terry Rutkowski of the WisDOT were responsible for the coordination and administrative management of the project. The authors would like to acknowledge the assistance of Mr. Gerald Rienke of Mathy Construction Co., Inc. for his role in construction of test sections and assistance in installing the field instrumentation for this project. Special acknowledgments are also due to the following individuals: Mr. Bill Shepherd, Materials Engineering, Wisconsin Department of Transportation (WisDOT) District 5, Mr. John Volker, Chief Product Quality Management Engineer of WisDOT, and Mr. Kurt Johnson of the Research Division.

EXECUTIVE SUMMARY

This project was initiated by the Pavement Research Unit of the Wisconsin Department of Transportation (WisDOT) as a result of concerns regarding excessive premature cracking of asphaltic pavements. The objectives of the project were to field validate the Superpave™ binder specification criteria and to field validate the pavement temperature estimation procedure used in the current version of the Superpave™ software.

In order to investigate the relation between asphalt binder properties and the cold temperature premature cracking, six test sections were constructed on USH 53 in Trempealeau County. The test sections were similar in type of mixture and pavement structure but varied in the type of asphalt cement used in the surface layer and the binder layer. The asphalts used in the study included two modified asphalts and one control unmodified asphalt. The grades of the modified asphalts were PG 58-34 and PG 58-40. The unmodified asphalt was a 120-150 penetration grade asphalt.

Field instrumentation was installed in two of the test sections to record thermal data in the atmosphere and the pavement. The instrumentation was used specifically to monitor the temperature of the test sections as a function of time and depth from the pavement surface. A meteorological station was also assembled at the test site to monitor the weather conditions including the air temperature.

The pavement instrumentation included four pavement temperature probes. These probes were similar to the probes recommended by the Long-Term Pavement Performance (LTPP) program as described in the "Seasonal Monitoring Program Guidelines." A stainless-steel temperature probe and a fiberglass temperature probe were used for each of the two test sections to provide the needed redundancy and to evaluate if the conductivity of the temperature probe affects measurements. The meteorological data collected included air temperature, relative humidity, wind speed and direction, and solar radiation.

Pavement surface conditions were inspected periodically to monitor the appearance of thermal cracks or other types of cracks. Asphalt samples were tested for detailed rheological and failure properties as recommended by Superpave™ protocols.

This report includes analysis of the data collected during the first 22 months of the project. The analysis was focused on development of a statistical model for estimation of pavement low and high temperature from meteorological data. The model was compared to the Superpave recommended model and to the more recent model recommended by LTPP program. The temperature data analysis indicates that there is a strong agreement between the new model and the LTPP model for the estimation of low pavement design temperature. The analysis, however, indicates that the LTPP model and the Superpave™ model underestimate the high pavement design temperature at air temperatures higher than 30 °C. The temperature data analyses also indicate that there are significant differences between the standard deviation of air temperatures and the standard deviation of the pavement temperatures. These differences raises some questions about the accuracy of the reliability estimates used in the current Superpave™ recommendations.

The report also includes the results of the surface condition surveys and its relation to the properties of the asphalts used in the test sections. Significant differences in severity of reflective cracking were observed. No strong correlations could be found with properties of the asphalt binders used. The pavement performance analysis could not be used for evaluating the Superpave binder criteria because all sections suffered from reflective cracking. The results could not be used to verify the criteria limits because these limits were established to control thermal cracking rather than reflective cracking. The results indicate that the modified binders used in this study did not result in reduction of reflective cracking. This finding questions the value of the modified binders in reduction of reflective cracking.

Based on the statistical analysis of pavement and weather data the following models have been selected. They are referred to in this report as the Wisconsin pavement temperature models:

- WI Minimum Pavement Design Temperature Model:

$$T_{PAV(MIN)@surface} = -1.102 + 0.425\, T_{AIR(MIN)} + 0.362\, Tavg$$

where $T_{PAV(MIN)@surface}$ = the minimum pavement temperature at the surface;

$T_{AIR(MIN)}$ = the minimum air temperature; and

Tavg = the average air temperature during the 24 hours preceding the time at which minimum pavement temperature was measured.

This model should be used only when the minimum air temperature is lower than - 5°C. This model has a value of R^2 of 95.9 % and a standard error of estimate of 1.22 °C.

- WI Maximum Pavement Design Temperature Model:

$$T_{PAV@20mm(MAX)} = -8.424 + 0.710\sqrt[4]{Solar_{-0} * T^2_{AIR(MAX)}} + 0.485\,T_{AIR-01} + 0.259\sqrt[4]{Solar_{-0} * MS_{-0}}$$

where $T_{PAV@SURFACE(MAX)}$ = Maximum pavement temperature at 20 mm depth, °C;

$T_{AIR(MAX)}$ = Maximum air temperature, °C;

$Solar_{-0}$ = Daily total solar radiation intensity, Watt/m^2; and

MS_{-0} = Daily peak of solar radiation intensity, Watt/m^2.

This model should be used when the pavement temperature at 20 mm depth is above 40 °C. This model has an R^2 value of 91.60% and a standard error of estimate of 1.87 °C.

TABLE OF CONTENTS

LIST OF FIGURES

LIST OF TABLES

CHAPTER ONE
INTRODUCTION

1.1 Introduction

This research report includes the findings to date of the research project entitled "Investigation of Modified Asphalt Performance Using SHRP Binder Specification." The project was initiated by the Pavement Research Unit of the Wisconsin Department of Transportation (WisDOT) as a result of concerns regarding excessive premature cracking of asphaltic pavements. Several test sections were constructed in 1995 on USH 53 in Trempealeau County, Wisconsin. The test sections were similar in type of mixture and pavement structure but varied in the type of asphalt cement used in the surface layer and the binder layer. Neat and polymer modified asphalts that meet different grades of the Strategic Highway Research Program (SHRP) specification were used in these sections. The test sections were also instrumented with temperature sensors at four locations to monitor the temperature of the test sections as a function of depth from the pavement surface. A weather station was also assembled at the test site to simultaneously monitor the weather conditions including the air temperature.

The objectives of the project were to field validate the Superpave™ binder specification and to field validate the pavement temperature estimation procedure used in the current version of the Superpave™ software. The project is planned to continue for five years with continuous monitoring of temperature and weather conditions and with periodic monitoring of pavement performance.

The report includes four chapters in addition to this introductory chapter. Chapter Two covers the field instrumentation and the data collection system used. Chapter Three includes the analysis of the temperature data and Chapter Four includes the analysis of binder properties and its relation to observed performance. Chapter Five includes the research findings, study recommendations, and the implementation plan. The report also includes three appendices that cover the background of Superpave™ procedures, data files details, and binder testing procedures.

1.2 Research Objectives

Based upon the concerns of excessive premature cracking and the recent advent of SHRP designed asphalt binders, both the Wisconsin Department of Transportation (WisDOT) and the industry felt it opportune to conduct a research investigation to evaluate a modified mix using the new SHRP asphalt cement (AC) binder specifications. It was decided that research should be directed at evaluating the ability to improve the cold weather performance of the asphaltic mix designs through:

1. *Field validation and calibration of the Superpave™ binder specification criteria.*

   By monitoring the performance of well controlled test sections subject to different climatic and traffic conditions, and by extensive characterization of properties of binders used in these sections, the criteria of the Superpave™ binder specification can be validated. The data collected can also be used to calibrate the limits in the binder specification, if necessary. With this validation and calibration, the implementation of the specification will lead to better designed AC pavements for Wisconsin.

2. *Field validation of the pavement temperature estimation procedure used in the current version of the* Superpave™ *software.*

   By instrumenting the pavement sections with thermal sensors along the depth of the pavement layers, the temperature pavement can be measured continuously with time. These measurements can be used, with air temperatures measured simultaneously, to verify the temperature estimation procedure. Without such validation, users of Superpave software will run the risk of specifying asphalt using the wrong pavement temperatures. This can increase the cost of binders or compromise the quality of designed pavement.

1.3 Superpave™ Performance-Based Asphalt Binder Specification and Pavement Temperature Estimation Procedures

The new Superpave™ asphalt binder specification uses the designation *PG x-y* to grade the binders, where

PG = Performance Graded;

x = high pavement design temperature (° C); and

y = low pavement design temperature (° C).

The design temperatures are estimated using weather data assembled in a weather database that is part of the Superpave™ system. The background of the procedure for estimation is included in Appendix A of this report.

As an example, a PG 52-40 grade is designed to be used in an environment which experiences a maximum design pavement temperature of 52° C and a minimum of -40° C.

The grades are specified primarily for a specific combination of traffic loading and environmental conditions. The loading condition related to high temperature performance is a vehicle speed of 100 km/h and a traffic volume of less than 10^7 equivalent single axle loads (ESALs). Environmental conditions are specified in terms of

- average 7-day maximum pavement design temperature; and
- minimum pavement design temperature.

The average 7-day maximum pavement design is the average of the highest daily pavement temperatures for the 7 hottest days in a year. The lowest annual pavement temperature is the coldest pavement temperature of the year. The maximum design pavement temperature is determined at 20 mm below the pavement surface and the minimum design pavement temperature is determined at pavement surface.

The high design pavement temperature at specified depth, d, is calculated using the following equation (Kennedy et al. 1994):

$$T_{d(max)} = [T_{s(max)} + 17.8][1 - 2.48 \cdot 10^{-3} d + 1.085 \cdot 10^{-2} d^2 - 2.441 \cdot 10^{-8} d^3] - 17.8 \quad (1.1)$$

where

$T_{d(max)}$ = maximum pavement temperature at depth d, ° C;

$T_{s(max)}$ = maximum pavement surface temperature, ° C; and

d = depth from surface, mm.

Substituting the design depth, d = 20 mm, Equation 1.3 can be simplified to:

$$T_{20(\max)} = 0.955\, T_{s(\max)} - 0.8 \qquad (1.2)$$

where

$T_{20(max)}$ = maximum pavement temperature at 20 mm, °C

$T_{s(max)}$ = maximum pavement surface temperature, °C

Superpave™ defines the minimum pavement surface temperature as the minimum air temperature. Since the low design pavement temperature is determined at the pavement surface, the low design pavement temperature is the assumed to be the lowest annual air temperature.

The minimum pavement temperature at a specified depth, d, is calculated using the following equation (Kennedy et al. 1994):

$$T_{d(min)} = T_{s(min)} + 5.1 \cdot 10^{-2}\, d - 6.3 \cdot 10^{-5}\, d^2 \qquad (1.3)$$

where

$T_{d(min)}$ = minimum pavement temperature at depth d, °C;

$T_{s(min)}$ = minimum pavement temperature at surface, °C;

d = depth from surface, mm.

In addition to the Superpave™ models, the LTPP recently developed new revised models for high and low pavement temperatures. These models were developed using a linear regression method. Models were judged based on the R^2-value, the variability, and their boundary condition. The high pavement temperature model can be written as follows (Mohseni 1996):

$$T_{d(max)} = 30.36 + 0.780854\, T_{a(max)} - 0.002750\, \phi^2 - 1.615427\, d \qquad (1.4)$$

where

$T_{d(max)}$ = maximum pavement temperature below surface, °C;

$T_{a(max)}$ = maximum air temperature, °C;

ϕ = Latitude of the section, (° Latitude) ; and

d = Depth to surface, mm.

A model for low pavement temperature is similar to the high temperature model adding $T_{a(min)} \cdot d$ term in the model. The resulting model is shown below (Mohseni 1996).

$$T_{d(min)} = 7.69 + 0.71215\, T_{a(min)} - 0.003694\, \phi^2 + 0.7821\, d + 0.00615\, T_{a(min)} \cdot d \qquad (1.5)$$

where

$T_{d(min)}$ = minimum pavement temperature at depth d below surface, ^{o}C;

$T_{a(min)}$ = minimum air temperature, ^{o}C.

There are significant differences between the Superpave™ models and the LTPP models. These models are compared to the results of this study in detail in Chapter Three.

CHAPTER TWO

FIELD INSTRUMENTATION AND DATA COLLECTION SYSTEM

2.1 Research Project Description

The research project is a 11.33 km section of USH 53. The section is located in Trempealeau County, Wisconsin, beginning from Whitehall and going north to Pigeon Falls. The project consisted of cracking and seating of the existing Portland cement concrete (PCC) pavement and overlaying it with 102 to 114 mm MV (Medium Volume) type asphalt concrete pavement including a 38 mm surface course. The overlaying project was constructed in August 1994; The pavement temperature instrumentation system and weather station were installed in December, 1994.

The USH 53 PCC pavement was constructed in 1948. It was a 6.10 m wide non-reinforced Portland cement concrete pavement with joint spacing of 6.10 m, including 2.40 m crushed aggregate shoulders. The pavement section consisted of 200 mm PCC surface course, 80 mm crushed aggregate base course, and 300-460 mm of sand fill. In 1992, 610 mm asphaltic concrete shoulders were added. USH 53 is functionally classified as minor arterial with an Average Daily Traffic (ADT) of 4100 vehicles in 1995 and an estimated 5000 ADT by 2015. Truck traffic is estimated to be 11.3% of ADT.

Six test sections were constructed on this section of USH 53. Each test section was constructed to a length of approximate 1,220 m. All test sections were designed using the current WisDOT asphalt mix specification for Medium Volume Roadway (MV). Variations were made to the specification for the asphalt binder to include SHRP performance grade binders including modified asphalt binders. Details of each test section are listed in Table 2.1, and illustrated in Figure 2.1 on the following page.

Table 2.1 List of the USH 53 Test Sections

Section (1)	Location (2)	Surface Course (3)	Binder Course (4)
Test Section 1	Sta. 090+00 to 130+00	Pen 120-150	Pen 120-150
Test Section 2	Sta. 130+00 to 170+00	PG 58-34	Pen 120-150
Test Section 3	Sta. 170+00 to 210+00	PG 58-34	PG 58-34
Test Section 4	Sta. 210+00 to 250+00	PG 58-40	PG 58-34
Test Section 5	Sta. 250+00 to 290+00	PG 58-40	PG 58-40
Test Section 6	Sta. 290+00 to 330+00	PG 58-40	Pen 120-150

* Test Section 1 is a control section. The Pen 120-150 AC is roughly equivalent to a SHRP PG 58-28.

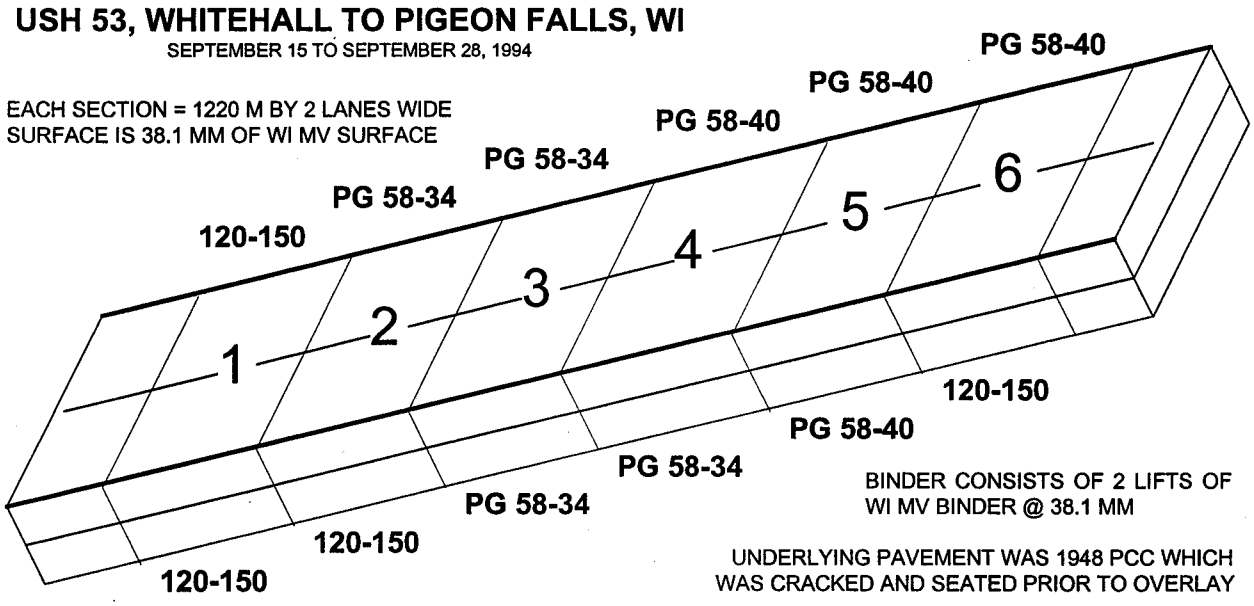

Figure 2.1 USH 53 Test Sections

2.2 Description of Data Collection System

The data collection system included pavement temperature monitoring, climatological monitoring, data acquisition and control computer (DACC), and remote telecommunication equipment. Two test sections, test section 3 (referred as Box 1) and test section 4 (referred as Box 2), were selected for the pavement temperature monitoring system. The sections were selected arbitrarily such that the temperature sensors are close enough to be connected to the telecommunication boxes. These boxes were placed on the side of the road close to the sensors yet outside the safety section of the road. One of the telecommunication boxes was mounted on the weather data collection tower. The tower was installed to mount the climatological monitoring system. The schematic system of DACC and its relation to power supply, remote telecommunications, and instrumentation is shown in Figure 2.2.

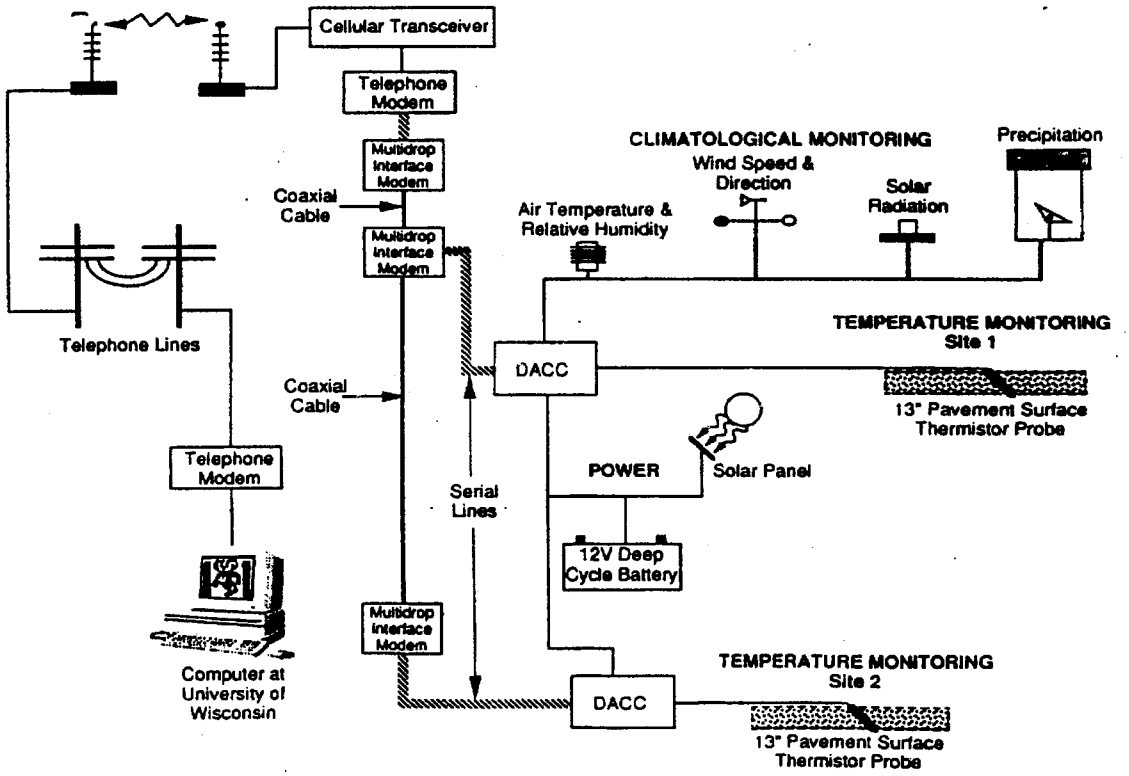

Figure 2.2 Schematic of DACC and Relationship to Power Source, Telecommunication, and Instrumentation (adapted from Benson et al. 1994)

2.2.1 *Pavement Temperature Monitoring System*

The temperature sensor selected for this project is the thermistor. Thermistors are thermally sensitive resistors (usually made of semiconductor material) with an extremely large temperature coefficient of resistance. Very small changes in temperature result in large changes in resistance (hundreds of thousands of ohms) which can be directly related to changes in temperature.

Four thermistor probes similar to ones used and recommended by the LTPP program were installed at two locations within the pavement test section. These probes are manufactured by Measurement Research Corporation (MRC) and were designed to measure the temperature at four depths within pavement layer. The schematic illustration of these probes is shown in Figure 2.3.

Because of concerns regarding the conductivity of the probes, two types of probes were used. A stainless steel probe, similar in design to the LTPP design, and a fiberglass thermal probe were placed in each of the two test sections being instrumented to provide redundant measurements. Using two different types of probes allows evaluating the effect of probe conductivity on sensor readings. In addition, one set of three thermocouples was installed in one of the sections for comparative purposes.

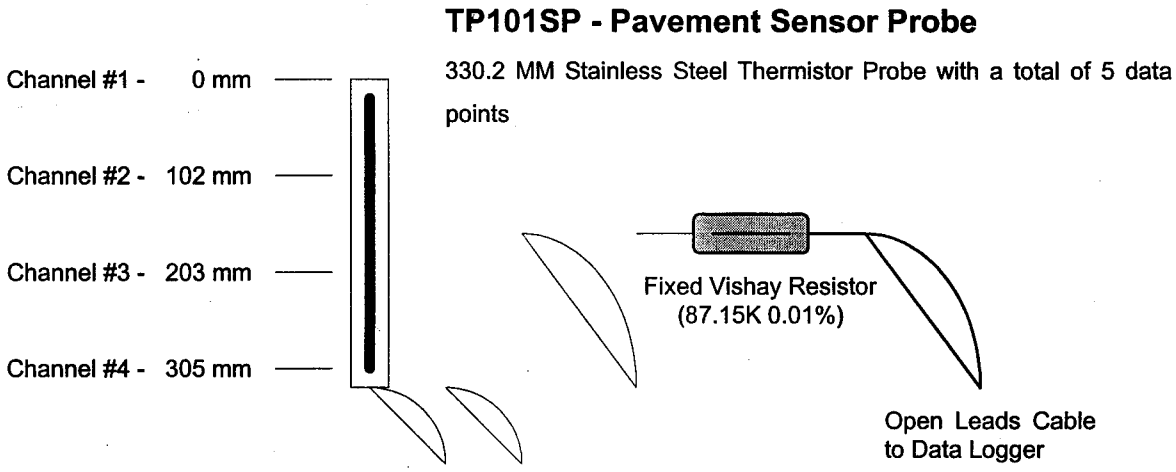

Figure 2.3 Pavement Thermal Probe Recommended by The LTPP

The probes were installed at the center of the north bound lane, 76.2 m and 64 m from the joint between two consecutive sections, and in longitudinal cuts parallel to the center line of the pavement sections. Transverse cuts were made to carry the instrumental cables to the outside edge of the pavement. The probes were placed at an angle such that the top end is 6.4mm below the surface. Such placement enables the probes to measure pavement temperatures at four depths: 6.4 mm, 38.1 mm, 69.9 mm, and 101.6 mm below the surface.

The probes in each section were spaced 3.048 m apart to avoid the possibility of weakening the pavement section. Each probe had its own cable that extending in an independent trench to the side of the road and connects to the cable trench. This was done to minimize the possibility of having a complete loss of measuring capability in case one cable was damaged.

A schematic illustration of the thermal probes location and details of the instrumentation layout is shown in Figure 2.4. The profile of the thermal probe installed in pavement section is shown in Figure 2.5.

2.2.2 Climatogical Monitoring System

In addition to the pavement temperature monitoring system, climatological data (including air temperature, relative humidity, wind speed and direction, and solar radiation) are being monitored. This data were being collected to evaluate the effects of these environmental factors on the thermal variations of the pavement. Instruments used for each measurement are summarized in Table 2.2. The air temperature and relative humidity instruments are housed in a radiation shield to minimized the effects of solar radiation.

2.2.3 Data Acquisition and Control Computer and Telecommunication Device

A Data Acquisition and Control Computer (DACC) was designed for continuous monitoring of sensors. It was capable of recording signals from a number of different physical transducers to condition these signals, perform an analog-to-digital (A/D)

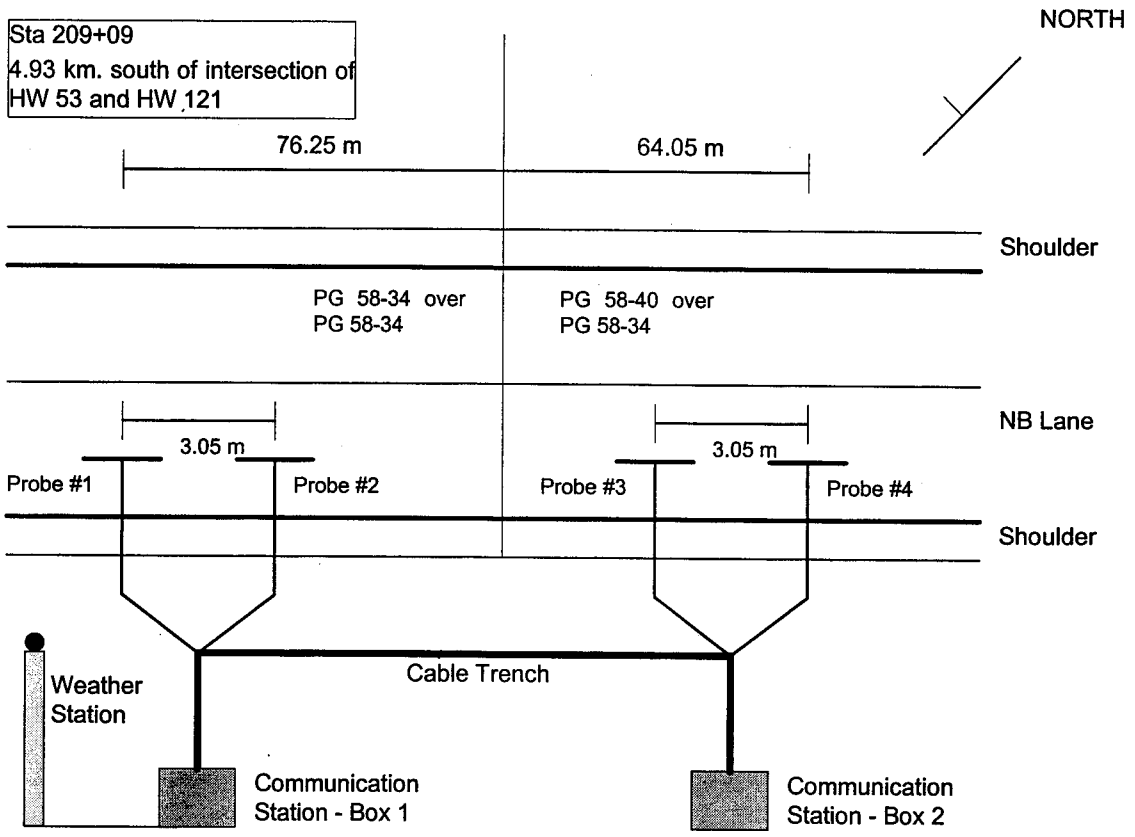

Figure 2.4 Location of Thermal Probes and Details of the Instrumentation Layout

Table 2.2 Climatological Instruments

Climatological Measurement (1)	**Instrument** (2)	**Output signal** (3)
Air temperature	Thermistor	Resistance (excitation with voltage measurement)
Relative humidity	Capacitive relative humidity sensor	Excitation with voltage Measurement
Solar radiation	Silicon photo voltaic detector	Low level voltage (12mV max)
Wind speed	Anemometer	Low level a-c signal (frequency proportional to wind speed)
Wind direction	Potentionmeter wind vane	Resistance (excitation with voltage measurement)

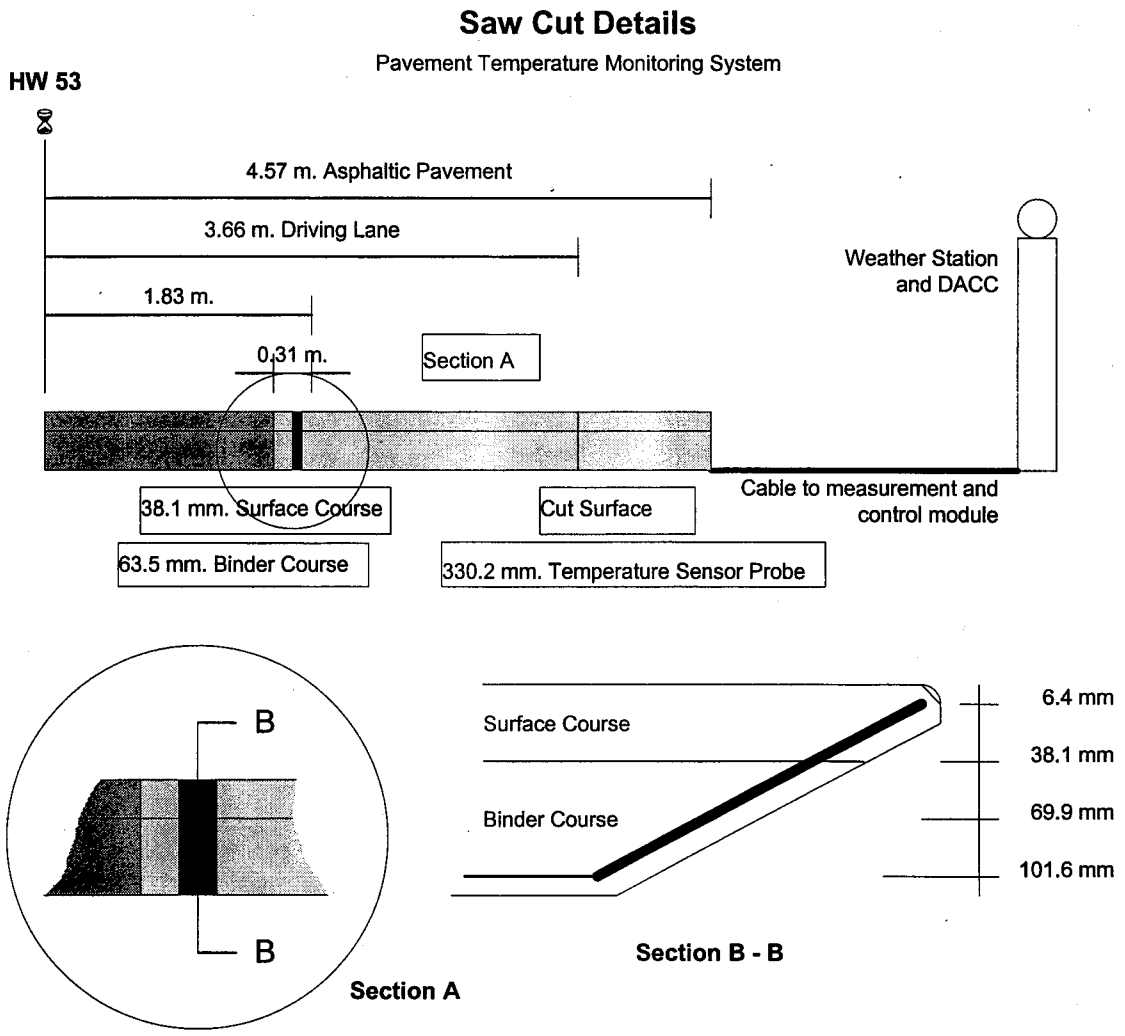

Figure 2.5 Schematic Diagram of Thermal Probe Installed in Pavement Section

conversion, and control equipment such as switches, valves, and multiplexers. It is also capable of processing raw data, saving important data and determining non-critical information to minimize the data storage space. This equipment works over a wide range of temperature (-55°C to 85°C), which might be experienced in Wisconsin.

Most of the sensors were wired directly to the DACC. The system is programmed to read the data from the pavement and weather sensors every hour, and then store the data collected. The system has a capacity to store approximately 60 days of data. This data can be accessed and downloaded by using a telecommunication device.

Telecommunications are completed via cellular telephone transmission. The system was programmed to be able to receive a remote call at certain periods of time for downloading or programming purposes. It was also programmed to call back and leave a message when the temperature drops below -20°C or when the temperature drop rate exceeds 2°C per hour. These limits could be changed to adjust to the typical temperature fluctuation in that area. The program automatically shuts down the telecommunication if it detects that the power is very low. However, due to the probe damage that occurred at one test section (from which the program read the data to determine the temperature and the drop rate), the call back system had been disabled since September 1995.

2.2.4 Power Source

Power for the system was provided by an 18 watt solar panel. Deep-cycle lead-acid batteries were used to provide power when the solar panels do not provide adequate output. In the beginning of March, 1995, a loss of communication occurred at test section three. A visit to the site and a detailed inspection of the system indicated that the power cable between the solar panel and weather data tower and the computer collecting data from the section was damaged. Consequently, the data was lost for a period of approximately four weeks. A solar panel assembly and battery were placed at the second box for that test section to avoid the recurrence of this incident.

2.3 Data Collection Procedure

The telecommunication system was programmed such that the cellular telephone was activated one hour every day in order to conserve power of the system. During that hour, selected to be between 10:00am to 11:00am CST, the data collected could be downloaded from the site computer to the computer at UW-Madison. This time window could be changed to a different time period by modifying the program. Each of the two instrumented sections had its own computer memory and collected different sets of data. At the weather data tower, the computer collected the climatological data in addition to the pavement temperature data. The data collection system was programmed to collect one reading from each sensor every hour.

The details of the data files and samples of data collected are shown in appendix B. The data collected were used to analyze the relation between the weather data and the temperature of the pavement layers.

CHAPTER THREE

PAVEMENT TEMPERATURE DATA ANALYSIS

3.1 Data Analysis

This chapter includes the analysis of the data collected from the pavement instrumentation system and the weather station during the first 22 months of the research project (12-94 to 9-96). It is divided into several sections to discuss the different factors and to show the statistical relationship between the pavement temperature and the weather data.

3.1.1 Effect of Temperature Probe Material

One concern at the beginning of the research project was whether or not the temperature probe's conductivity would affect the measurement of the pavement temperature. To study this effect, two probes made of two different materials were installed in each test section (Figure 2.4, page 11). One set of probes installed was made of stainless steel and the other set was made of fiberglass. Both are similar in dimension and specification. Compared to the fiberglass, stainless steel is a high thermal conducting material. The data from probes were statistically compared and analyzed to determine if the probe conductivity has a significant effect on the pavement temperature measurements.

Figures 3.1 to 3.4 show the relationships between the pavement temperatures measured by the stainless steel probe and the pavement temperatures measured by the fiberglass probe. The relationships include the data from the thermistors at 6.4 mm and 101.6 mm below the surface, at each location. In this analysis, the 6.4 mm layer is referred as surface layer and the 101.6 mm layer is referred as bottom layer.

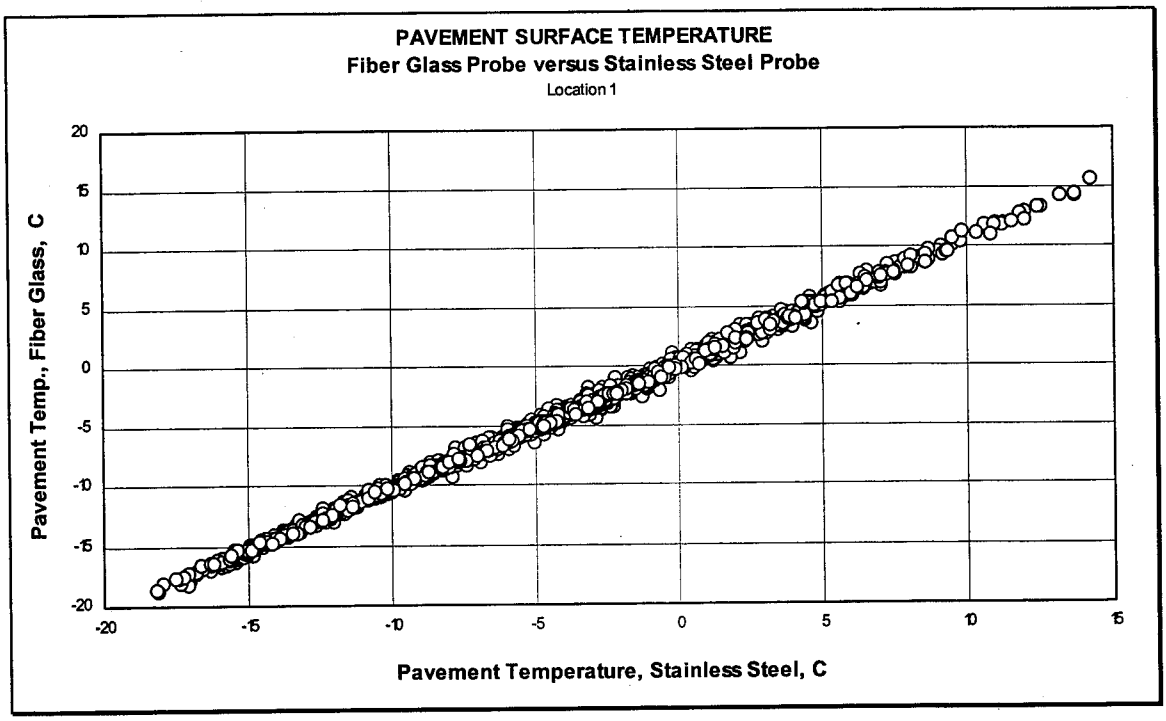

Figure 3.1 Relationship of Pavement Temperature Measurements at Surface Layer for Stainless Steel and Fiberglass Probe at Box 1

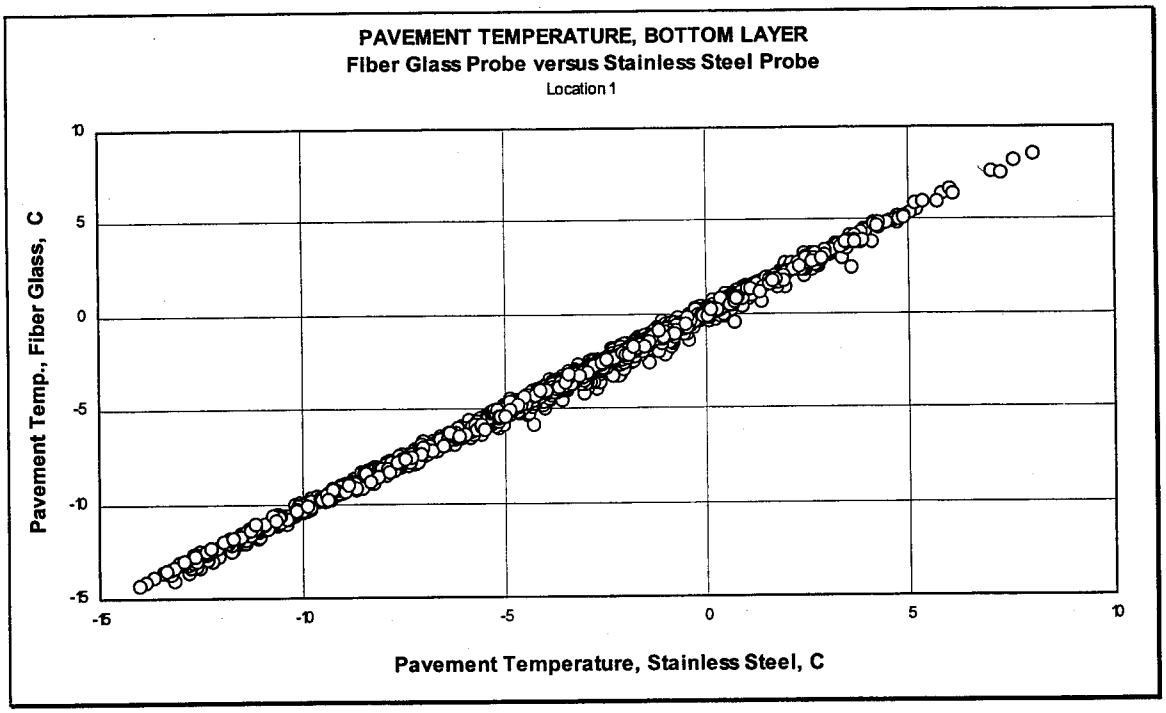

Figure 3.2-- Pavement Temperature Measurements at Bottom Layer for Stainless Steel and Fiberglass Probes at Box 1

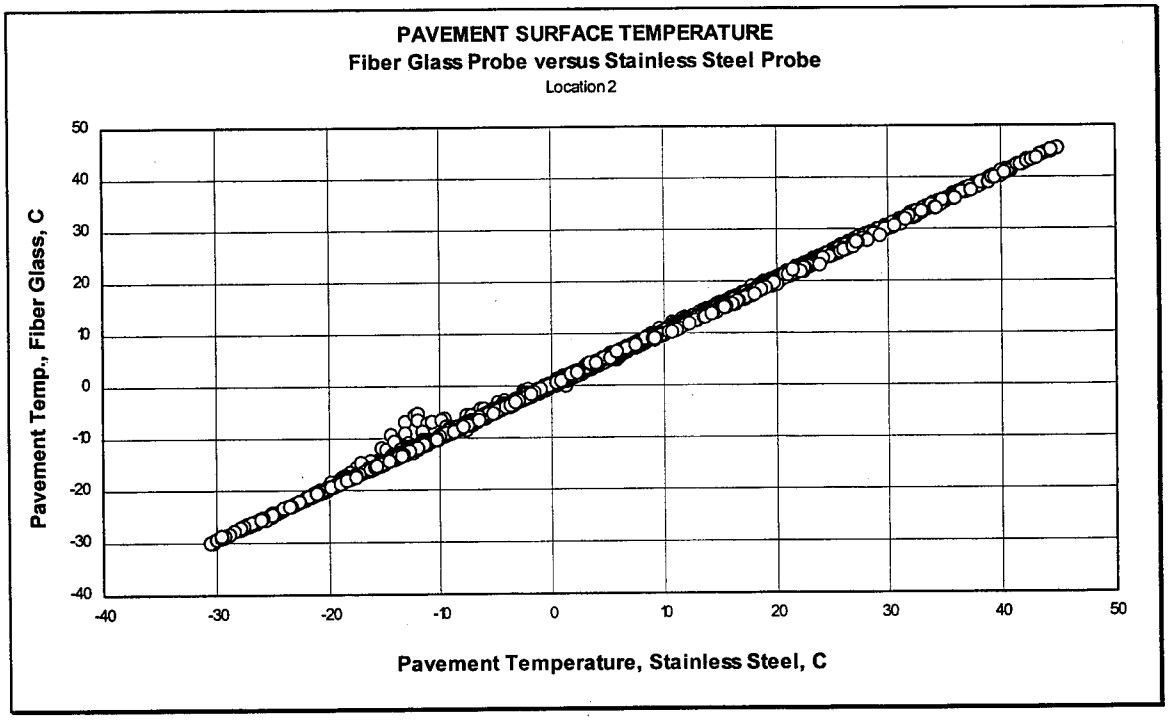

Figure 3.3 Pavement Temperature Measurements at Surface Layer for Stainless Steel and Fiberglass Probe at Box 2

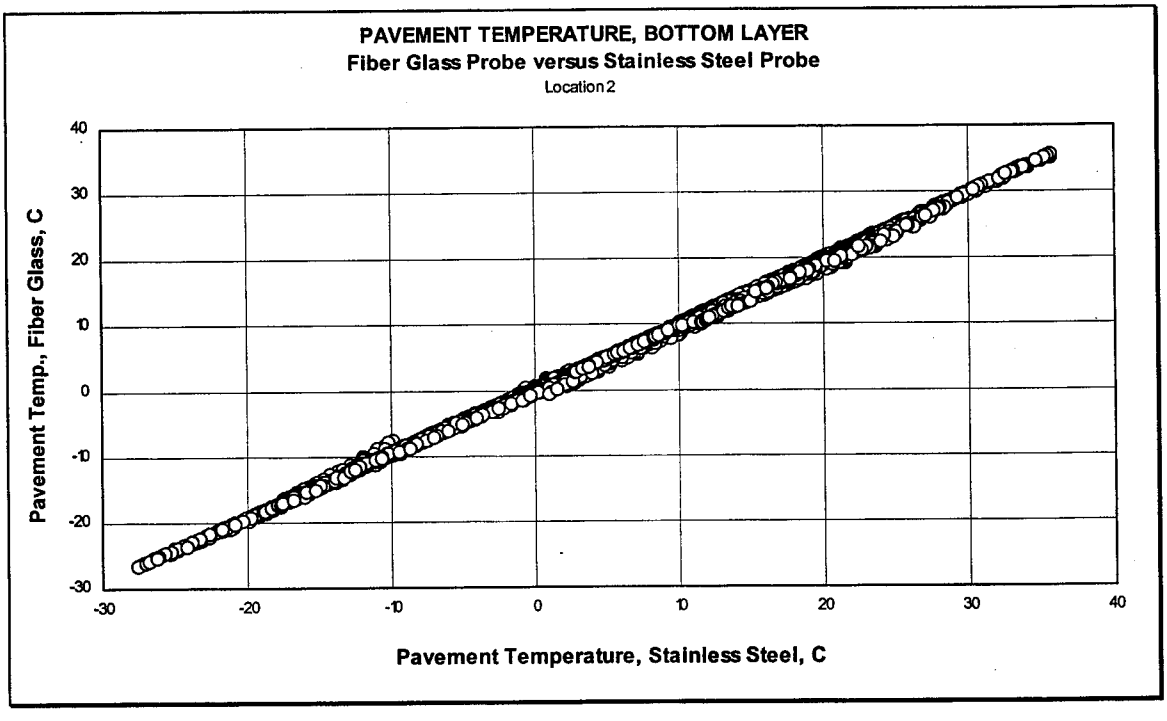

Figure 3.4 Pavement Temperature Measurements at Bottom Layer for Stainless Steel and Fiberglass Probes at Box 2

The data collected from Box 2 in test section four (shown in Figure 3.3 and 3.4) covered a wider range of temperature than Box 1 in test section three, because at Box 1 the pavement temperature data was only collected for the first 10 months of the project, while at Box 2 data was collected for the first 22 months. The plots show that the relationships between the two probes follow a linear model, which is close to the equality line (the line forming a 45^{o} angle with both axes). There are, however, small variations observed in all graphs indicating that a statistical analysis is needed to determine if these variations have a significant effect on the temperature measurements.

A simple regression equation was fitted for each data set to establish a functional relationship between probes' measurements. The regression parameters, b_1 and b_0 are estimated from the regression. The parameter b_1 represents the slope of the equation and b_0 represents the intercept of the regression equation. The values of the slope and the intercept are used to test the null hypothesis $H_0(b_1=1.0 \text{ and } b_0=0)$ against the alternative $H_A(b_1\neq1.0 \text{ and } b_0\neq0)$. The test is conducted by comparing the observed *t-value* with the appropriate tabulated critical t at the certain confidence coefficient $(1-\alpha)$. It the *t-test* is significant, the equation will be $(y=x)$ meaning that the effect of the different probes can be neglected.

The summary of the regression analysis is presented in Table 3.1. The table also includes the index R^2, which is interpreted as the proportion of total variability in y that is explained by x, and the *Standard Deviation, s*. The s will be used to estimate the standard deviation of the slope and the intercept to test the hypotheses.

The result of the linear regression analysis shows that there are small differences observed between the stainless steel and the fiber-glass probes' measurements, at both layers and at both locations. The slopes of the regression equation range between 0.96 to 1.006 and the intercepts range between $-0.202^{o}C$ to $-0.096^{o}C$.

The combination of slope and intercept indicates that there is one temperature for each equation where the stainless steel and the fiberglass probe show the same temperature. At Box 1, the temperatures meet at $-3.7^{o}C$ at surface and $-2.4^{o}C$ at bottom layer. Below these temperatures, the stainless steel probe shows a higher temperature than the fiberglass probe and vice versa. At Box 2, which collected much more data than Box 1, the

Table 3.1 Summary of Regression Analysis on Pavement Temperature Differences between Two Types of Probes

		Linear Regression Equation	St. Dev.	R^2
Box 1	Surface Layer	Stainless Steel = - 0.144 + 0.961 Fiber Glass	0.3141	99.7 %
	Bottom Layer	Stainless Steel = - 0.096 + 0.960 Fiber Glass	0.2342	99.6 %
Box 2	Surface Layer	Stainless Steel = - 0.202 + 0.998 Fiber Glass	0.3173	99.9 %
	Bottom Layer	Stainless Steel = - 0.183 + 1.006 Fiber Glass	0.3669	99.9 %

Note: Box 2 covered pavement temperature data for the first 22 months of the research project, and Box 1 only covered for the first 10 months due to temperature probes damage on August 1995.

relationship is different. At the surface layer, the stainless steel probe shows a lower temperature than the fiberglass probe at all temperatures. However, at the bottom layer, the stainless steel probe shows a lower temperature than the fiberglass probe when the temperature exceeds +18.3°C.

The summary of the *t-test* result of each equation is shown in Table 3.2. The table includes the *t-value* calculated from each equation and also the critical *t* at 95% confidence level. The results show that all observed *t-value* exceed the critical *t-value*, suggesting that the null hypothesis $H_0(b_1=1.0 \text{ and } b_0=0)$ is rejected. The rejection means that, statistically, the temperature measurements between the stainless steel and the fiberglass probe are not the same and the different probe conductivity significantly affects the temperature measurements.

The difference in temperature measurements can be attributed to the fact that the depth of the probes may be slightly different. Although the probes were installed as precisely as possible, the differences could have resulted from the inability to place each probe in the exact same depth, especially during the process of covering with the paving material.

Table 3.2 Summary of *t-test* of The Linear Regression Equation

			b's	s.e. of *b*'s	*t-value*	Critical *t*
Box 1	Surface Layer	Slope	0.961	0.001248	31.25	1.64
		Intercept	- 0.144	0.008609	16.78	
	Bottom Layer	Slope	0.960	0.001378	29.03	1.64
		Intercept	- 0.096	0.007091	13.53	
Box 2	Surface Layer	Slope	0.998	0.000182	10.99	1.64
		Intercept	- 0.202	0.003523	57.24	
	Bottom Layer	Slope	1.006	0.000200	30.00	1.64
		Intercept	- 0.183	0.004109	44.45	

The temperature difference between the stainless steel and the fiberglass probe measurements ranges between -0.85°C and +0.55°C (negative sign means that the stainless steel probe measurement is lower than the fiberglass probe measurement) at the 95% confidence level. These differences are very small and can be neglected for practical purposes. Therefore, the pavement temperature used in further analysis is the average pavement temperature from all four probes.

3.1.2 Statistical Analysis

Statistical regression analysis is an effective method for obtaining mathematical equations that describe the observed dependence of one variable on another. The method of least squares was used in the analysis of the data in this study. This method is the basis of the regression analysis that can give the best estimates of the regression coefficients that constitute the regression model (Draper 1966).

3.1.2.1 Regression Analysis on Daily Minimum Pavement Temperatures

Figure 3.5 shows the relationship between the daily minimum pavement temperature measured 6.4 mm below surface and the daily minimum air temperature. As evident in the figure, there is a strong correlation between the pavement temperature and the daily minimum air temperature. The figure shows that the relationship is not a straight line and

that a wide range of pavement temperatures can be observed for a given air temperature. This indicates that there are other factors, besides the minimum air temperature, that affects the pavement temperature. Linear regression analysis was used to establish the model defining the minimum pavement temperature measured at 6.4 mm below the pavement surface as a function of the minimum air temperature and the other weather factors measured in this study.

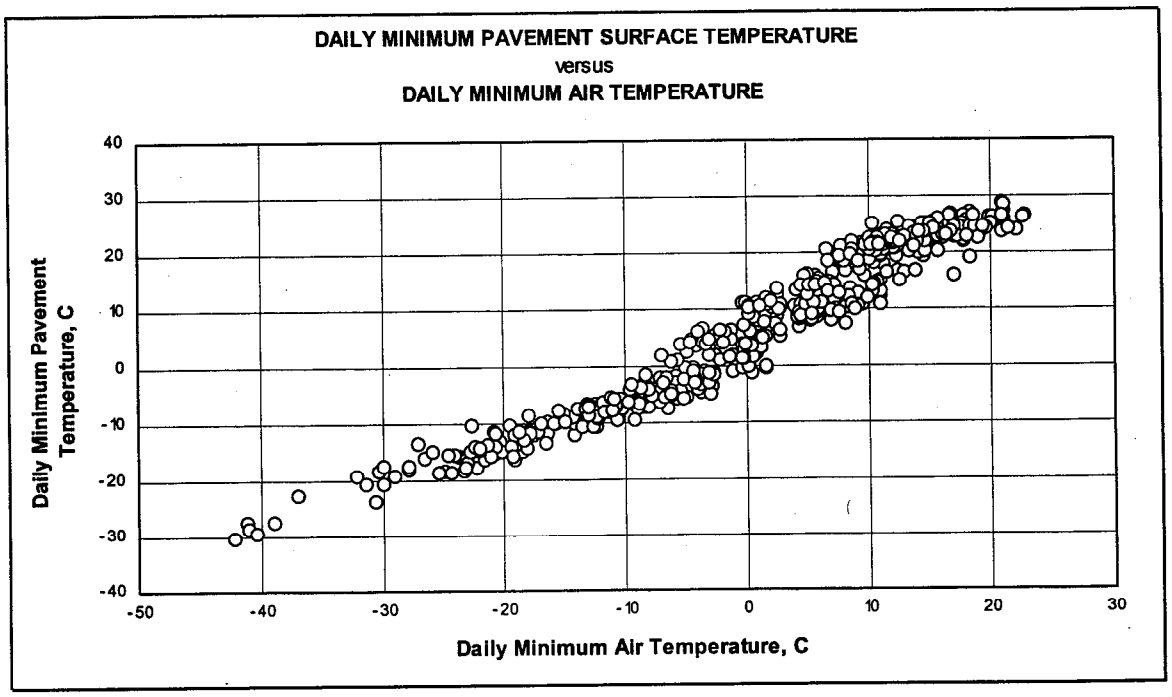

Figure 3.5 Daily Minimum Pavement Temperatures at 6.4 mm plotted versus Daily Minimum Air Temperatures

Several models were considered including a linear, a bi-linear model, and also a second order polynomial model. The best low temperature model recommended (equations 3.1 and 3.2) was a bi-linear model divided at 0°C for air temperature.

$$T_{PAV@6.4mm(MIN)} = 2.27 + 0.778\, T_{AIR(MIN)}, \quad \text{for air temperature} < 0^{\circ}C; \text{ and} \qquad (3.1)$$

$$T_{PAV@6.4mm(MIN)} = 6.83 + 1.014\, T_{AIR(MIN)}, \quad \text{for air temperature} > 0^{\circ}C; \qquad (3.2)$$

where $T_{PAV@6.4mm(MIN)}$ = Minimum pavement temperature at 6.4 mm, °C; and

$T_{AIR(MIN)}$ = Minimum air temperature, °C.

The R^2 value for this model is 96.3% and the standard deviation of estimate is 2.714 °C. The standard deviation is relatively high which suggests that the model had to be improved by adding new parameters in addition to the minimum air temperature, or by changing the type of model.

After considering several options it was decided that an indicator of the thermal cycle and solar intensity experienced by the pavement for the past several days is a promising option. On this basis, the parameters T_{AIR-01} and $Solar_{-1}$ were introduced. T_{AIR-01} is the average air temperature calculated during the 24 hours preceding the time at which the minimum pavement temperature occurred. $Solar_{-1}$ is the total solar radiation intensity calculated during the 24 hours preceding the time at which the minimum pavement temperature occurred (unit = Watt/m^2). It was also believed that an interaction parameter between the total solar radiation intensity and the air temperature is needed. The fourth root of the interaction ($\sqrt[4]{F_{123} * S_1}$) was chosen on the basis of the theory that any blackbody surface above absolute zero radiates heat at a rate proportional to the fourth power of the absolute temperature from the heat transfer model for radiation (Kreith 1958). "S_1" is $Solar_{-1}$ and "F" is the average hourly freezing index of the air temperature. F_{123} is calculated by adding the hourly air temperature below 0°C during the 72 hours preceding the time the pavement temperature reaches its daily minimum temperature, and dividing the total by 72 (the number of hours for three days).

Several other combinations between F and ***Solar*** were considered into the analysis including F_1, F_2, $\boldsymbol{Solar}_{-2}$, and $\boldsymbol{Solar}_{-3}$. It appeared that these combinations are not significant enough to enter the model.

Since the main focus in the low temperature model is to establish the model for minimum annual pavement temperature, a stepwise regression analysis was conducted for the data of daily minimum pavement surface temperatures when the daily minimum air temperature is below 0°C. The results are shown in Table 3.3.

Adding $\boldsymbol{T}_{AIR\text{-}01}$ decreased the standard deviation from 1.91 to 1.65 (the standard deviation of the bi-linear model was 2.714). Although thermal history of pavement appears to improve prediction of pavement temperature from air temperature, the model standard deviation (ranges between 1.32 and 1.91) was considered relatively high. To further improve the model, the data included in the model was limited to lower temperatures. Table 3.3 also shows the results of the stepwise regression analysis involving the data when the daily minimum air temperatures are below -5°C. At this temperature range, the minimum pavement temperature at 6.4 mm is usually below 0°C. This limitation is reasonable since most of the yearly minimum pavement temperature is expected below 0°C (Superpave™ uses -10°C as the highest minimum design pavement temperature).

Table 3.3 Stepwise Regression Models on Minimum Pavement Temperatures at 6.4 mm when Air Temperatures < $0^{O}C$

Step	$T_{PAV@6.4mm(MIN)}$ = Const.	$T_{AIR(MIN)}$	T_{AIR-01}	$Solar_{-1}$	$^{4}VF_{123}*S_1$	s (2)	R^2 (3)
	Model (1) Tair < 0°C						
1.	-2.1867	0.882				1.91	93.40
2.	-0.4681	0.603	0.273			1.65	95.10
3.	-1.2362	0.547	0.315	0.00041		1.53	95.79
4.	1.5934	0.303	0.396	0.00081	-0.445	1.25	97.20
	Model (2) Tair < -5°C						
1.	0.377	0.687				1.727	91.68
2.	-3.165		0.805			1.734	91.73
3.	-1.001	0.422	0.359			1.222	95.92
4.	-1.461	0.410	0.370	0.00025		1.176	96.66
5.	0.262	0.297	0.405	0.00053	-0.268	1.115	96.81

The results show that limiting the model to a lower temperature range results in better prediction. Since the Superpave™ weather database consists of the minimum air temperature only, the first model shown in Table 3.3 (section 2) is recommended for use with conjunction to the Superpave™ database. Note that this model should only be used when the air temperature is below $-5^{O}C$. The model is

$$T_{PAV@6.4m(MIN)} = 0.3768 + 0.687\ T_{AIR(MIN)} \qquad (3.3)$$

The model with the thermal history factor can be used if a complete weather database is available. This is the best recommended model because the model produces a low standard deviation compared to the first model. The reduction of standard deviation (from 1.73 for Model 1 to 1.22 for Model 3) indicates that thermal history of the pavement significantly affects the pavement temperature and results in a better estimate of the minimum pavement temperature. If solar radiation data is available, the fourth model provides an even better estimate. The recommended low temperature model without solar radiation is

$$T_{PAV@6.4mm(MIN)} = -1.001 + 0.422\,T_{AIR(MIN)} + 0.359\,T_{AIR-01} \quad (3.4)$$

where $T_{PAV@6.4mm(MIN)}$ = Minimum pavement temperature at 6.4 mm, °C;

$T_{AIR(MIN)}$ = Minimum air temperature, °C; and

T_{AIR-01} = Average air temperature during the 24 hours before the time the minimum air temperature is measured, °C.

The residual plots of both recommended models (Equation 3.5 and 3.6) are shown in Figures 3.6 and 3.7. Both plots tend to have funnel-shape distributions, fanning out with the predicted values which indicates that the variance of the residuals is not constant. However, further examination on the data points distribution suggests that the trend is primarily caused by an unbalanced data points at certain temperature range (There are only 11 data points at the temperature range below -20°C compare to 150's at the range above -20 °C). The models are therefore considered acceptable.

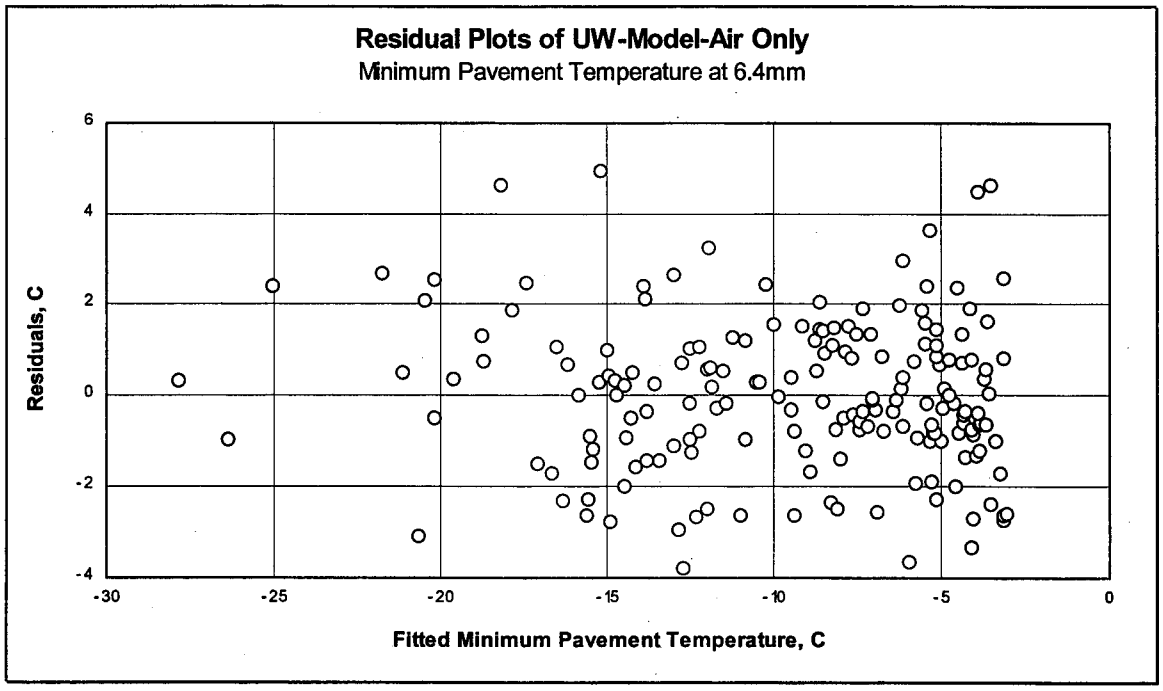

Figure 3.6 Residual Plot of the UW Low Temperature Model Involving Air Temperature Only

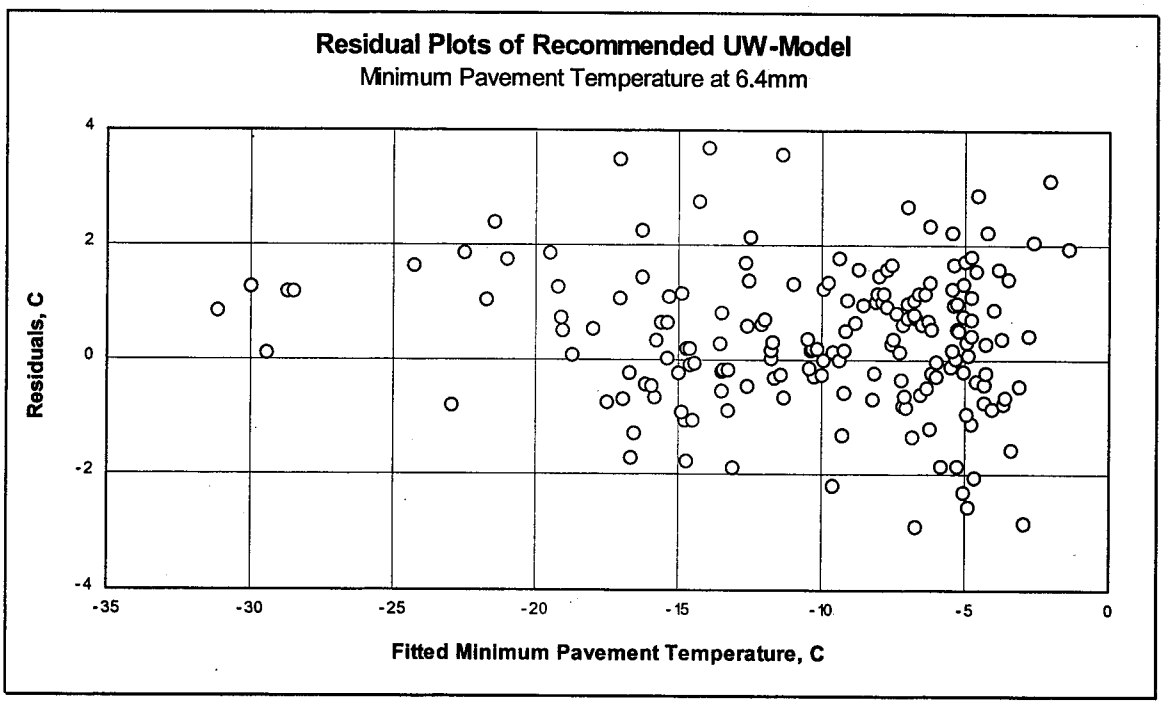

Figure 3.7 Residual Plot of the Best Recommended UW Low Temperature Model

3.1.2.2 Analysis of Minimum Pavement Temperature at a Specified Depth

The pavement temperature at 6.4 mm was used as a predictor variable to estimate the pavement temperature at different depths. Several forms of depth (d) were considered as parameters including d, d^2, d^3, $\sqrt{d}$, and the interaction between pavement temperature and these forms of the depth parameter. A stepwise regression analysis was applied to select the best regression equation. The minimum pavement temperature at a specified depth can be calculated using the following equation:

$$T_{d(MIN)} = T_{PAV@6.4mm(MIN)} - \left[0.00123 T_{PAV@6.4mm(MIN)} (d - 6.4)\right] + 0.0146 (d - 6.4) \quad (3.5)$$

where $T_{d(MIN)}$ = Minimum pavement temperature at depth d, °C;

$T_{6.4mm(MIN)}$ = Minimum pavement temperature at 6.4 mm, °C; and

d = Depth from surface, mm.

The standard deviation of the regression equation is 0.563. It should be noted that the data used to develop Equation 3.7 include the daily minimum pavement temperatures measured by each thermistor of the probes. The analysis assumes that all the minimums occur at the same time. Also the relationship is limited to the estimate of the pavement temperature when air temperature is lower than -5°C.

Superpave™ defines the minimum pavement design temperature at pavement surface. Substituting Equations 3.3 into Equation 3.5 and using 0.0 mm as the d yields

$$T_{PAV@SURFACE(MIN)} = 0.286 + 0.692\, T_{AIR(MIN)} \quad (3.6)$$

and substituting Equations 3.4 into Equation 3.5 yields

$$T_{PAV@SURFACE(MIN)} = -1.102 + 0.425\, T_{AIR(MIN)} + 0.362\, T_{AIR-01} \quad (3.7)$$

where $T_{PAV@SURFACE(MIN)}$ = Minimum pavement temperature at surface, °C.

Equation 3.6 is recommended for use in conjunction to the Superpave™ weather database and Equation 3.7 is the best recommended model if a complete weather database is

available. Notice that these equations are only used when the minimum air temperature is below -5°C.

3.1.2.3 Regression Analysis on Daily Maximum Pavement Temperatures

Superpave™ binder specification also provides an equation to estimate the maximum pavement temperature. Unlike the minimum design pavement temperature, the maximum design pavement temperature is calculated from the 7-hottest day air temperature within the year. In this research project, the analysis was conducted to relate the daily maximum pavement temperature at 6.4 mm to the daily maximum air temperature and other weather factors.

Figure 3.8 shows the relationship between daily maximum pavement temperatures at 6.4 mm and daily maximum air temperatures. A strong correlation is observed. Similar to the one observed in the daily minimum temperature (Figure 3.5), a wide range of pavement temperatures at a single air temperature is observed.

The data analysis resulted in selecting a bi-linear model with pavement surface temperature at 10°C as the intersection point for the model. The recommended high temperature models were as follows:

$$T_{PAV@6.4mm(MAX)} = -0.519 + 0.820\, T_{AIR(MAX)} + 0.00335\, Solar_{-0}, \quad \text{for pavement temperature} < 10^{\circ}\text{C; and} \tag{3.8}$$

$$T_{PAV@6.4mm(MAX)} = 2.811 + 1.087\, T_{AIR(MAX)} + 0.00246\, Solar_{-0}, \quad \text{for pavement temperature} > 10^{\circ}\text{C.} \tag{3.9}$$

where $T_{PAV@6.4mm(MAX)}$ = Maximum pavement temperature at 6.4 mm, °C;

$T_{AIR(MAX)}$ = Maximum air temperature, °C; and

$Solar_{-0}$ = Daily total solar radiation intensity, Watt/m².

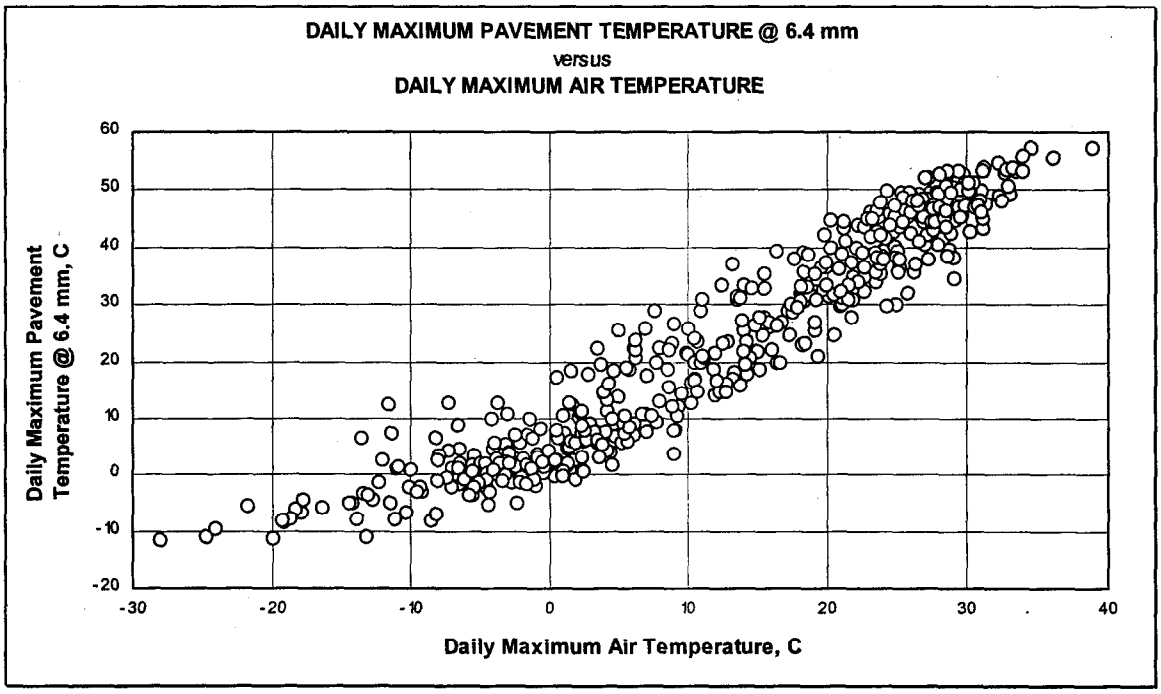

Figure 3.8 Relation between Daily Maximum Pavement Temperatures at 6.4 mm and Daily Maximum Air Temperatures

Since the maximum air temperatures are mostly higher than 10 °C, Equation 3.9 is the recommended model for the high temperature model. The total daily solar radiation is calculated by adding the solar radiation intensity recorded every hour within a particular day together. The R^2 of the bi-linear model is 98.2% and the standard deviation is 2.606 °C. The high standard deviation motivated the search for a better model. The new analysis was focused on the pavement temperature above 30 °C. This limit was chosen because the Superpave specification starts the binder grade at the maximum design pavement temperature of 46°C.

Derivatives of parameters used in the bi-linear model were developed. They included the fourth root of $\boldsymbol{Solar_{-0}}$, and the fourth root of the interaction between $\boldsymbol{Solar_{-0}}$ and the square of maximum air temperature. Also, $T_{AIR\text{-}01}$ as an indicator of the thermal history of the pavement is also included.

New parameter *"MS (Maximum Solar)"* is introduced. *MS* is the daily peak of solar radiation intensity. It is used in combination with $\boldsymbol{Solar_{-0}}$ because the combination provides a better representation of weather condition. For instance (in one occasion), two different days

with almost the same maximum air temperature and daily total of solar radiation, yet had a different maximum pavement temperatures. Further analysis indicated that the daily peaks of solar radiation intensity on those particular days were different resulting in the different maximum pavement temperatures. The analysis also showed that low total solar radiation with high daily peak and high total with low daily peak had the same effect on the maximum pavement temperatures.

The results of the stepwise regression analysis are shown in Table 3.4. The results indicate that the model prediction is significantly improved when the solar radiation parameter enters the model. The recommended model is shown in Equation 3.10.

Table 3.4 Stepwise Regression Models on Maximum Pavement Temperatures at 6.4 mm Involving Air Temperature > 20^{O}C

	Model (1)							s (2)	R^2 (3)
	$T_{PAV(MAX)}$ =								
	Const.	$T_{AIR(MAX)}$	$^4VS_0 \cdot T_A^2$	T_{AIR-01}	$^4VS_0 * MS$	$Solar_1$	Solar 0		
1.	8.509	1.337						4.443	52.09
2.	5.712	0.972					0.00231	2.632	83.10
2.	-3.562		1.088					2.646	83.02
3.	-6.443		0.977	0.409				2.036	89.93
4.	-8.428		0.716	0.489	0.261			1.865	91.60
5.	-8.618		0.691	0.476	0.261	2.8E-4		1.808	92.13

$$T_{PAV@6.4mm(MAX)} = -8.428 + 0.716\sqrt[4]{Solar_{-0} * T_{AIR(MAX)}^2} + 0.489\,T_{AIR-01} + 0.261\sqrt[4]{Solar_{-0} * MS_{-0}} \quad (3.10)$$

where T_{AIR-01} = Average air temperature at day one before to the day of the minimum air temperature, ^{O}C; and

MS_{-0} = Daily peak of solar radiation intensity, Watt/m^2.

This finding clarifies that solar radiation has a great effect on the maximum pavement temperature variation. Similar to the low temperature model, the fourth root of solar radiation was selected on the basis of heat transfer theory for radiation.

The residuals plot for this model is shown in Figure 3.9. Similar to the low temperature models, the plot tends to have a funnel-shape distribution, but fanning in with the predicted values. Further analysis indicates that the trend is primarily caused by an insufficient number of data points collected, especially at the temperature range above 50°C.

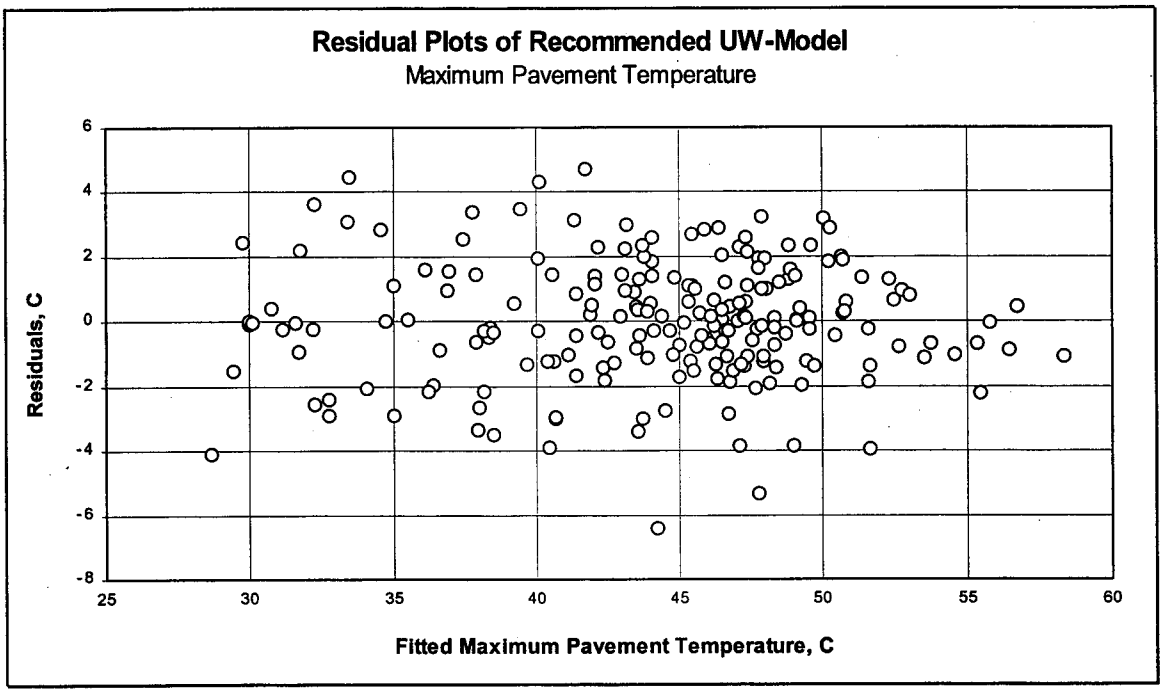

Figure 3.9 Residual Plot of the Recommended UW High Temperature Model

For comparison with models introduced by SHRP and LTPP, the second model with solar radiation can be used. If ($Solar_0$) is assumed equivalent to latitude in these models, the following equation is recommended:

$$T_{PAV@6.4mm(MAX)} = 2.811 + 1.087\, T_{AIR(MAX)} + 0.00246\, Solar_{-0}, \qquad (3.11)$$

3.1.2.4 Analysis of Maximum Pavement Temperatures at Specified Depth

The maximum pavement temperature at a specified depth is calculated using the following equation. The model was determined using the stepwise regression procedure.

$$T_{d(MAX)} = T_{PAV@6.4mm(MAX)} - 2.68 \times 10^{-3} (d - 6.4) T_{PAV@6.4mm(MAX)} + 4.25 \times 10^{-4} (d - 6.4)^2 \quad (3.12)$$

where $T_{d(MAX)}$ = Maximum pavement temperature at depth d, °C;

$T_{PAV@6.4mm(MAX)}$ = Maximum pavement temperature at 6.4 mm, °C; and

d = Depth from surface, mm.

The statistics of the regression analysis are not as good as the model for low temperature. The R^2 is 93.54% and the standard deviation is 0.935. The equation is used only to estimate the pavement temperature when the maximum air temperature is above 25°C.

Superpave™ protocols use the design depth of 20 mm below the surface to determine the maximum design pavement temperature. Substituting Equation 3.11 into Equation 3.12 and using 20 mm as the depth d, yields

$$T_{PAV@20mm(MAX)} = -8.042 + 0.690 \sqrt[4]{Solar_{-0} * T^2_{AIR(MAX)}} + 0.471 T_{AIR-01} + 0.251 \sqrt[4]{Solar_{-0} * MS_{-0}} \quad (3.13)$$

where

$T_{PAV@20mm(MAX)}$ = Maximum pavement temperature at 20mm., °C.

Notice that equation 3.13 is only used when the maximum air temperature is higher than 30°C.

3.1.3 Statistics of Pavement Temperature and Weather Data

Weather data are monitored to examine their effects on pavement temperature. Air temperature, relative humidity, solar radiation, wind speed, and wind direction are the parameters that are considered to have an effect on pavement temperature. Tables C.1 through C.7 in Appendix C are prepared to show the general trends of these data during the first 22 months. Studying the statistics results in several important observations:

3.1.3.1. Daily Minimum Pavement Temperature

The minimum pavement surface temperatures are always higher than the minimum air temperatures. The monthly average difference ranges between 2.6°C to 11.3°C. Notice that the standard deviation of the minimum pavement surface temperature is significantly lower than the standard deviation of the minimum air temperature, within the range of air temperatures below 10°C. At temperatures above 10°C, the standard deviation of minimum pavement surface temperature is lower than the air temperature, but it is not as much as the temperatures below 10°C. The lower standard deviations of the pavement temperatures within the low temperature range reflects the dampening effect of the pavement layer mass on the temperature fluctuation.

3.1.3.2. Daily Maximum Pavement Temperature

Similar to the trends observed for the minimum pavement surface temperature, the monthly average of pavement temperature is higher than the average of air temperature. The magnitude of the difference ranges between 2.4°C and 20.5°C. However, the standard deviation of pavement temperature is higher than the standard deviation of air temperature. This finding can be related to the effect of solar radiation and the fact that solar radiation can increase the rate of temperature change in the pavement.

3.1.3.3. Temperature Difference between Surface and Bottom Layer

During the night, the bottom layer of the pavement experiences a higher temperature than the surface layer. The monthly average difference ranges between 2.4°C to 4.6°C. However, the difference reported can be as high as 7.7°C. On the contrary, during the day,

the surface layer experienced a higher temperature than the bottom layer. The average of the daily maximum difference ranges between 2.8°C and 10.1°C with the high of 13.3°C. Notice that the distance between the surface and bottom thermistor in the pavement is 95.2 mm. These initial readings indicate that the average difference is approximately 3.5°C per inch (25.4 mm) of pavement depth. It is important to note that the Superpave™ binder specification is based on standard grades that are spaced at 6°C interval.

3.1.3.4. Solar Radiation Intensity

Table 3.9 shows the statistics of solar radiation intensity. In includes the monthly low, high, average, and standard deviation of the daily peak of solar radiation intensity. The monthly average varies significantly with the month and is relatively low during winter and high during summer. The monthly average of daily peak solar radiation intensity ranges between 299 Watt/m2 and 908 Watt/m2 with the extreme low of 40.7 Watt/m2 in November 1995 and extreme high of 1279 Watt/m2 in June 1995. The total daily solar radiation also varies significantly. However, it is not always directly correlated to the daily peak solar radiation. The monthly total increases by more than 4 times between December and June. The total daily solar radiation is calculated by adding the solar radiation intensity recorded every hour within a particular day together. The hourly solar radiation data is the average of solar radiation intensity in one hour.

3.1.3.5. Air Temperature, Relative Humidity, Wind Speed and Direction

The monthly average of air temperature ranges between -13°C in December and 22.5°C in August. The monthly average of daily average relative humidity fluctuates between 65.7% and 87.5% with no specific trend. Wind speed ranges between 2.55 m/s and 6.2 m/s with the extreme maximum as high as 13.7 m/s recorded in March 1995. Wind direction is presented in percentage of occurrence, from North-East, East-West, South-West, and West-North. There is no specific trend observed in monthly average wind direction.

3.2 Validation of SHRP and LTPP Temperature Estimation Algorithm

The existing low and high temperature models used in Superpave™ binder specification and the Seasonal Asphaltic Concrete Pavement Temperature Models (SAPT) models developed by LTPP were compared to the recommended WisDOT models. Using the air temperature data, the pavement temperatures were calculated by applying these models. The predicted pavement temperatures were then plotted against the actual pavement temperatures measured at 6.4 mm from the surface. The relationships should indicate how well each model predicts the temperature variations.

3.2.1 Comparing the Low Temperature Models

SHRP considers the minimum pavement surface temperature as the minimum air temperature while LTPP uses an equation developed from the Seasonal Monitoring Program (SMP) Program (Equation 1.7). The result is shown in Figure 3.10. Since the actual pavement temperatures are measured at 6.4 mm below the surface, both SHRP and LTPP models were used for this depth. The latitude is also adjusted to match the location of the test sections (latitude = 44°). The WisDOT low temperature models used in this comparison are Equation 3.5 and Equation 3.6. Equation 3.5 is then referred to *"UW Recommended Low Temperature Model"* and Equation 3.6 is referred as *"UW Model Low Temperature Model with AIR only"*. The comparison is limited to include only the air temperature data when the minimum air temperature is below -5°C.

The ability of the model to explain the temperature variations is judged by the closeness of the correlation line to the equality line and by the standard deviation, *s*. The graph indicates that the SHRP model does not agree to the actual pavement temperature. The estimation is significantly lower than the actual pavement temperature. On the other hand, both WisDOT models and LTPP model show good temperature estimations with comparable standard errors of estimate. It is interesting to find this agreement between the LTPP model and the model developed using the Wisconsin data.

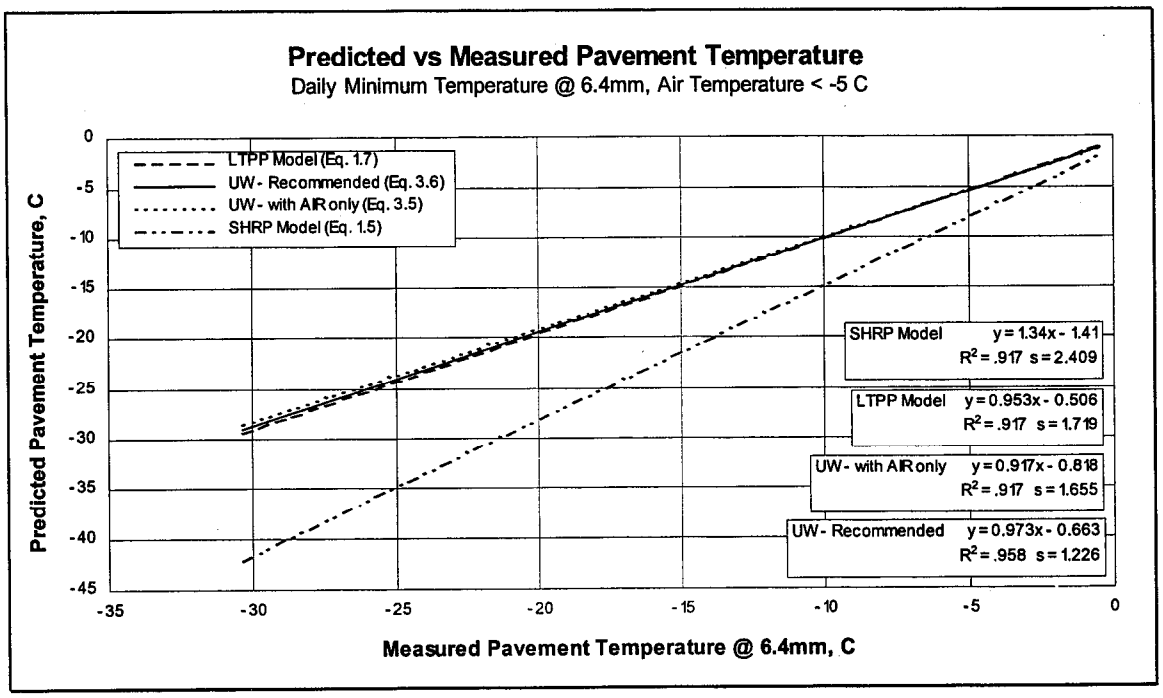

Figure 3.10 Comparison of Low Temperature Models

3.2.2 *Comparing the High Temperature Models*

The same procedure used for the low temperature models is applied to compare the high temperature models developed by SHRP, LTPP, and two WisDOT models, *"recommended"* and *"with AIR only"* . Similar to the low temperature model, the latitude and depth are set to 44° and 6.4 mm to correspond to the location of the test sections and the actual measured pavement temperatures. The comparison is limited to include only the data when the maximum air temperature is higher than 25°C. The result is presented in Figure 3.11.

Figure 3.11 shows that the recommended UW model is the best model to explain the temperature variations. It is indicated by the correlation line which is close to the equality line. The SHRP model tends to have a higher predicted temperature than measured below 50°C and significantly lower above 50°C. The LTPP model and the other UW model have almost parallel correlation lines but they do not have a good agreement with the equality line. Neither SHRP nor LTPP models incorporate solar radiation, but use latitude as the substitute. The latitude is constant because the data collected were from one location. This finding

strongly suggest that the effect of solar radiation cannot be neglected in predicting the maximum pavement temperature.

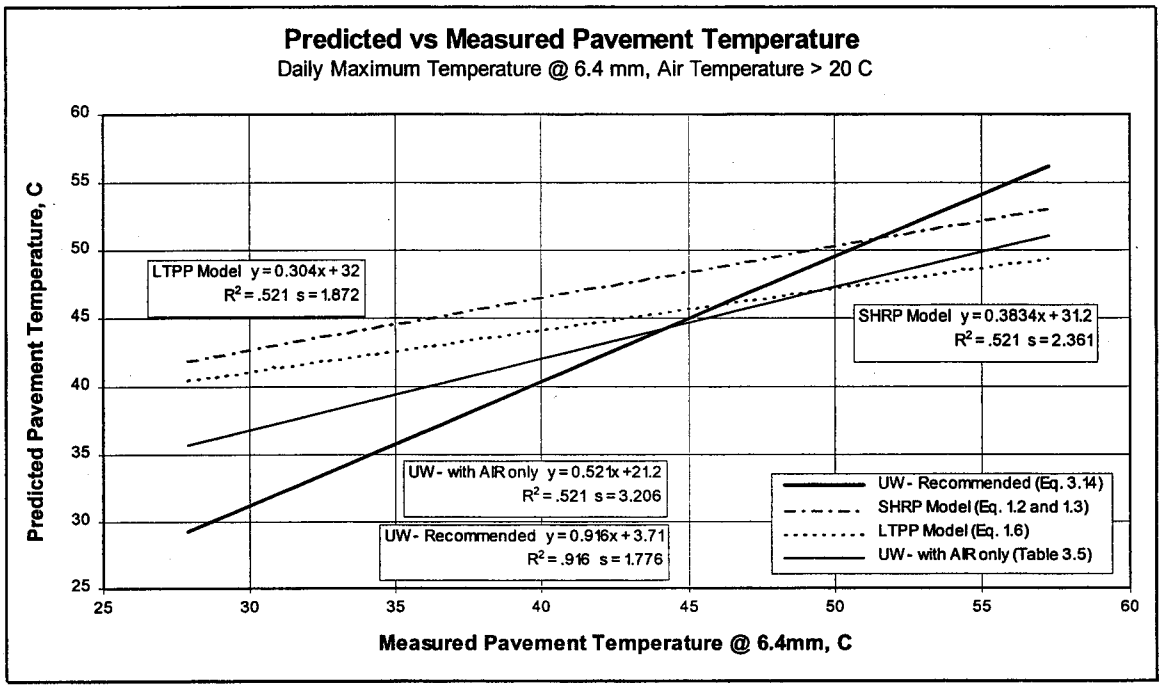

Figure 3.11 Comparison of High Temperature Models

3.2.3 *Standard Deviation of Air and Pavement Temperature*

Superpave™ assumes that the standard deviation of pavement temperature is equal to the standard deviation of air temperature. Data analysis does not confirm this assumption. Daily minimum and maximum of air and pavement temperatures are calculated and for each month, the average and the standard deviation of these temperatures are computed. The relationship between the standard deviation of pavement temperature and the standard deviation of air temperature is shown in Figure 3.12.

For the maximum temperatures the three hottest months of each of the two summers during which data were collected are shown. For the low temperature, the three coldest months for each winter were used. The relationships in the figure show that at high temperatures, the pavement temperature standard deviation is significantly higher than the standard deviation of the air temperature. For the low temperatures, the trend is reversed.

SHRP protocols use the standard deviation of air temperature to calculate the reliability factor in selecting the binder grade. The finding that pavement temperature variation is significantly different than air temperature have a significant impact on calculating the maximum and minimum design temperatures. The significance of this change depends on the level of the air temperature.

The following equations can be used to calculate standard deviation of pavement temperature from standard deviation of pavement temperature. Equation 3.14 is used for the minimum temperature and Equation 3.15 for the maximum temperature.

$$STDEV_{PAV(MIN)} = 1.170 + 0.6422\, STDEV_{AIR(MIN)} \tag{3.14}$$

$$STDEV_{PAV(MAX)} = 1.694 + 1.2733\, STDEV_{AIR(MAX)} \tag{3.15}$$

The equations are limited in use for minimum pavement surface temperature below $0^{o}C$ and maximum pavement surface temperature above $40^{o}C$.

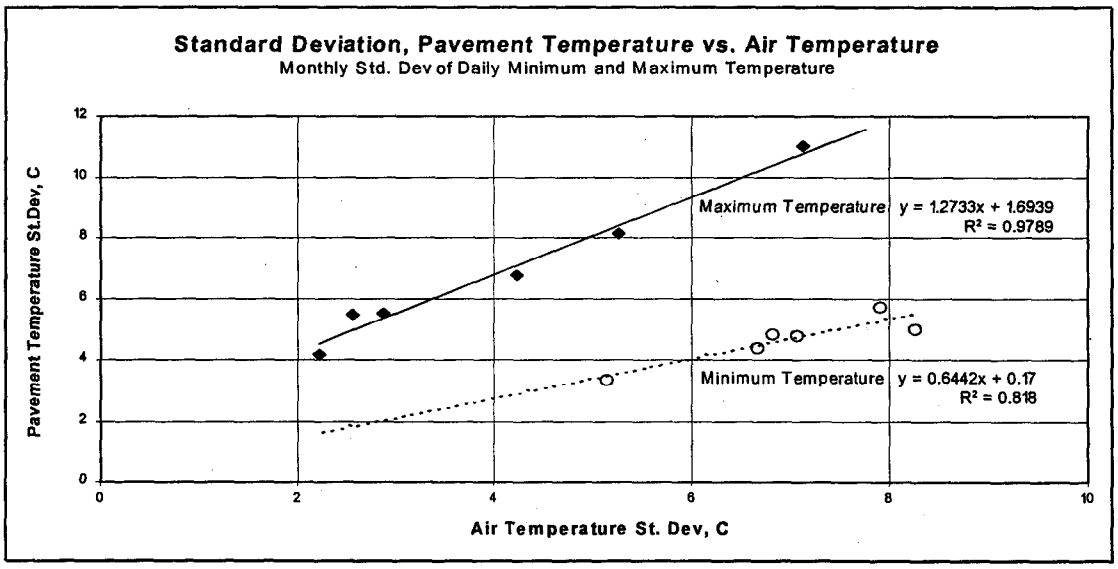

Figure 3.12 Comparison between Standard Deviation of Pavement Temperature and Standard Deviation of Air Temperature

Equation 3.15 is for the standard deviation of the daily maximum pavement temperature. It is important to note, however, that the Superpave™ protocols consider the 7-day average temperature as the pavement design temperature. Based on the 7-day average a

new set of standard deviations was calculated. Figure 3.13 gives the results, which show that the air and pavement 7-day average are very close and in general the pavement standard deviations are actually smaller than the air standard deviation. The following equation describes the relationship.

$$STDE_{PAV(Max)} = 0.1566 + 0.7102\ STDEV_{AIR(Max)} \tag{3.16}$$

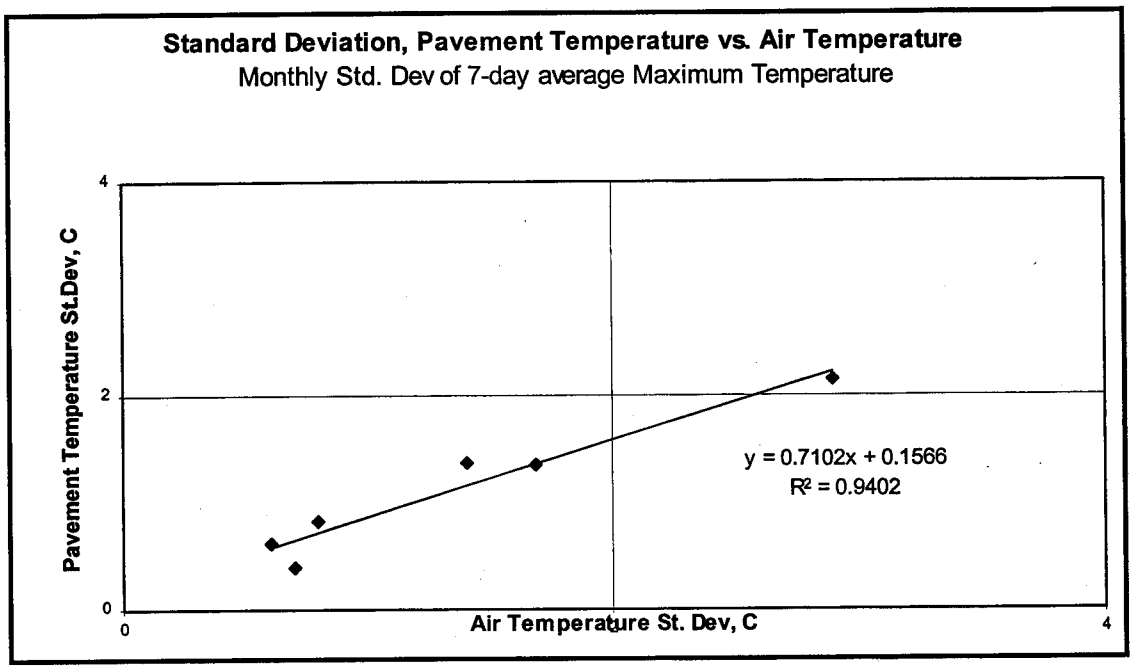

Figure 3.13 Comparison between Standard Deviation of 7-dayAverage Pavement Temperature and 7-day Average Standard Deviation of Air Temperature

3.2.4 Comparing Performance Grades Using WisDOT, LTPP, and SHRP Models

All 137 weather stations throughout Wisconsin as listed in the Superpave™ weather database were used in this analysis. The WisDOT, LTPP, and SHRP models were applied to the weather data to calculate the design temperatures and the grades. The resulting PG grades are listed in Table 3.12. The PG grades were determined at 50% and 98% reliability. SHRP and LTPP models were applied using the standard deviation of air temperature as the standard deviation of pavement temperature. The WisDOT model used Equation 3.15 and Equation 3.16 to estimate the standard deviation of pavement temperature. Since the Superpave™ weather database consists of only the minimum and maximum air temperature, the WisDOT models used are the models involving only air temperature (Equation 3.8 for minimum pavement temperature and Model 1 in Table 3.5 for maximum pavement temperature).

All low temperature grades have changed for both 50% and 98% reliability. At 50% reliability, 71 new PG grades (from 137 weather stations) are one grade higher and 66 are two grades higher than SHRP's. At 98% reliability, 56 are one grade higher, 80 are two grades higher, and only one is three grades higher. However, not all high temperature grades changed. As many as 62 PG grades at 50% reliability and 12 at 98% remain the same while the others increase by one grade when compared to the SHRP model. Compared to the LTPP, the WisDOT model shows that there are 25 counties for which the PG-grade has increased by two grades at the high temperature.

Table 3.12 UW, SHRP, and LTPP Pavement Temperatures and PG Grades for Wisconsin Weather Stations

COUNTY ID	WEATHER STATION	LAT	AIR TEMPERATURE LOW AVG	AIR TEMPERATURE LOW STD	AIR TEMPERATURE HIGH AVG	AIR TEMPERATURE HIGH STD	UW PAVEMENT TEMP. LOW AVG	UW PAVEMENT TEMP. LOW STD	UW PAVEMENT TEMP. HIGH AVG	UW PAVEMENT TEMP. HIGH STD	PAVEMENT TEMP. SHRP LOW	PAVEMENT TEMP. SHRP HIGH	PAVEMENT TEMP. LTPP LOW	PAVEMENT TEMP. LTPP HIGH	PG GRADE @ 50% REL. UW	PG GRADE @ 50% REL. SHRP	PG GRADE @ 50% REL. LTPP	PG GRADE @ 98% REL. UW	PG GRADE @ 98% REL. SHRP	PG GRADE @ 98% REL. LTPP
															HI LO	HI LO	HI LO	HI LO	HI LO	HI LO
BUFFALO	ALMA DAM 4	44.33	-30	4	32	2	-20.6	3.7	52.3	4.2	-30	51.2	-20.5	48.7	58 -22	52 -34	52 -22	64 -28	58 -40	58 -34
POLK	AMERY	45.30	-35	4	31	2	-24.0	3.7	50.9	4.2	-35	49.9	-24.4	47.7	52 -28	52 -40	52 -28	64 -34	58 -46	52 -34
LANGLADE	ANTIGO 1 SSW	45.13	-32	3	30	2	-22.0	3.1	49.5	4.2	-32	49.0	-22.2	46.9	52 -22	52 -34	52 -28	58 -34	58 -40	52 -34
OUTAGAMIE	APPLETON	44.25	-27	3	31	2	-18.5	3.1	50.9	4.2	-27	50.2	-18.3	47.9	52 -22	52 -28	52 -22	64 -28	58 -34	52 -28
COLUMBIA	ARLINGTON	43.33	-28	3	31	2	-19.2	3.1	50.9	4.2	-28	50.5	-18.7	48.1	52 -22	52 -28	52 -22	64 -28	58 -34	58 -28
COLUMBIA	ARLINGTON UNIV FARM	43.30	-29	3	32	2	-19.9	3.1	52.3	4.2	-29	51.5	-19.4	48.9	58 -22	52 -34	52 -22	64 -28	58 -40	58 -28
BAYFIELD	ASHLAND EXP FARM	46.57	-33	3	31	2	-22.6	3.1	50.9	4.2	-33	49.5	-23.4	47.3	52 -28	52 -34	52 -28	64 -34	58 -40	52 -34
SAUK	BARABOO	43.47	-32	4	32	2	-22.0	3.7	52.3	4.2	-32	51.4	-21.6	48.9	58 -22	52 -34	52 -22	64 -34	58 -40	58 -34
BAYFIELD	BAYFIELD 6 N	46.88	-19	4	29	2	-12.9	3.7	48.2	4.2	-19	47.5	-13.4	45.7	52 -16	52 -22	46 -16	58 -22	52 -28	52 -22
DODGE	BEAVER DAM	43.45	-28	4	32	1	-19.2	3.7	52.3	3.0	-28	51.4	-18.7	48.9	58 -22	52 -28	52 -22	64 -28	58 -40	52 -28
ROCK	BELOIT	42.50	-26	3	33	2	-17.8	3.1	53.6	4.2	-26	52.6	-17.0	49.9	58 -22	58 -28	52 -22	64 -28	58 -34	58 -28
VILAS	BIG SAINT GERMAIN DAM	45.92	-36	3	29	1	-24.7	3.1	48.2	3.0	-36	47.8	-25.3	45.9	52 -28	52 -40	46 -28	58 -34	52 -46	52 -34
TREMPEALEAU	BLAIR	44.30	-33	4	32	2	-22.6	3.7	52.3	4.2	-33	51.2	-22.6	48.7	58 -28	52 -34	52 -28	64 -34	58 -46	58 -34
CHIPPEWA	BLOOMER	45.10	-32	4	32	2	-22.0	3.7	52.3	4.2	-32	50.9	-22.2	48.5	58 -22	52 -34	52 -28	64 -34	58 -40	58 -34
SHAWANO	BOWLER	44.87	-32	4	30	2	-22.0	3.7	49.5	4.2	-32	49.1	-22.1	47.0	52 -22	52 -34	52 -28	58 -34	58 -40	52 -34
OCONTO	BREED 6 SSE	45.05	-33	4	32	2	-22.6	3.7	52.3	4.2	-33	50.9	-22.9	48.5	58 -28	52 -34	52 -28	64 -34	58 -46	58 -34
GREEN	BRODHEAD	42.62	-29	4	32	2	-19.9	3.7	52.3	4.2	-29	51.7	-19.2	49.1	58 -22	52 -34	52 -22	64 -28	58 -40	58 -28
FLORENCE	BRULE ISLAND	45.95	-35	4	30	2	-24.0	3.7	49.5	4.2	-35	48.7	-24.6	46.7	52 -28	52 -40	52 -28	58 -34	58 -46	52 -34
RACINE	BURLINGTON	42.67	-26	3	32	2	-17.8	3.1	52.3	4.2	-26	51.6	-17.1	49.1	58 -22	52 -28	52 -22	64 -28	58 -34	58 -28
MONROE	CASHTON	43.75	-27	7	31	2	-18.5	5.7	50.9	4.2	-27	50.4	-18.1	48.0	52 -22	52 -28	52 -22	64 -34	58 -46	52 -34
DANE	CHARMANY FARM	43.05	-28	4	32	2	-19.2	3.7	52.3	4.2	-28	51.5	-18.6	49.0	58 -22	52 -28	52 -22	64 -28	58 -40	58 -28
CALUMET	CHILTON	44.03	-28	3	32	2	-19.2	3.1	52.3	4.2	-28	51.2	-18.9	48.7	58 -22	52 -28	52 -22	64 -28	58 -34	58 -28
WAUPACA	CLINTONVILLE	44.62	-29	3	32	2	-19.9	3.1	52.3	4.2	-29	51.1	-19.8	48.6	58 -22	52 -34	52 -22	64 -28	58 -40	58 -28
PORTAGE	CODDINGTON 1 E	44.37	-34	3	31	2	-23.3	3.1	50.9	4.2	-34	50.2	-23.3	47.9	52 -28	52 -34	52 -28	64 -34	58 -40	52 -34
SAWYER	COUDERAY 7 W	45.87	-37	6	30	2	-25.4	5.0	49.5	4.2	-37	48.8	-26.0	46.7	52 -28	52 -40	52 -28	58 -40	58 -52	52 -40
MARINETTE	CRIVITZ HIGH FALLS	45.32	-32	4	31	2	-22.0	3.7	50.9	4.2	-32	49.9	-22.2	47.6	52 -22	52 -34	52 -28	64 -34	58 -40	52 -34
BARRON	CUMBERLAND	45.53	-34	3	31	2	-23.3	3.1	50.9	4.2	-34	49.8	-23.7	47.6	52 -28	52 -34	52 -28	64 -34	58 -40	52 -34
BURNETT	DANBURRY	46.02	-37	3	31	2	-25.4	3.1	50.9	4.2	-37	49.7	-26.0	47.5	52 -28	52 -40	52 -28	64 -34	58 -46	52 -34
LAFAYETTE	DARLINGTON	42.68	-30	4	33	2	-20.6	3.7	53.6	4.2	-30	52.6	-19.9	49.8	58 -22	58 -34	52 -22	64 -28	58 -40	58 -28
TREMPEALEAU	DODGE	44.13	-34	5	33	2	-23.3	4.4	53.6	4.2	-34	52.2	-23.3	49.5	58 -28	58 -34	52 -28	64 -34	58 -46	58 -34
IOWA	DODGEVILLE 1 NE	42.97	-28	3	31	2	-19.2	3.1	50.9	4.2	-28	50.6	-18.6	48.2	52 -22	52 -28	52 -22	64 -28	58 -34	58 -28
BAYFIELD	DRUMMOND	46.33	-34	5	31	2	-23.3	4.4	50.9	4.2	-34	49.6	-24.0	47.4	52 -28	52 -34	52 -28	64 -34	58 -46	52 -34
	EAU CLAIRE	44.82	-32	4	33	2	-22.0	3.7	53.6	4.2	-32	52.0	-22.1	49.3	58 -22	52 -34	52 -28	64 -34	58 -40	58 -34
CHIPPEWA	EAU CLAIRE FAA AP	44.87	-33	4	32	2	-22.6	3.7	52.3	4.2	-33	51.0	-22.8	48.5	58 -28	52 -34	52 -28	64 -34	58 -46	58 -34
FOND DU LAC	ELDORADO 1 SSWW	43.80	-28	4	32	2	-19.2	3.7	52.3	4.2	-28	51.3	-18.9	48.8	58 -22	52 -28	52 -22	64 -28	58 -40	58 -28
PIERCE	ELLSWORTH 1 E	44.73	-32	3	32	2	-22.0	3.1	52.3	4.2	-32	51.0	-22.0	48.6	58 -22	52 -34	52 -28	64 -34	58 -40	58 -28
EAU CLAIRE	FAIRCHILD RANGER STN	44.60	-31	3	31	2	-21.3	3.1	50.9	4.2	-31	50.1	-21.3	47.8	52 -22	52 -34	52 -22	64 -28	58 -40	52 -28
JEFFERSON	FORT ATKINSON	42.88	-28	4	32	2	-19.2	3.7	52.3	4.2	-28	51.6	-18.6	49.0	58 -22	52 -28	52 -22	64 -28	58 -40	58 -28
DOUGLAS	FOXBORO	46.50	-37	3	31	2	-25.4	3.1	50.9	4.2	-37	49.5	-26.2	47.3	52 -28	52 -40	52 -28	64 -34	58 -46	52 -34
VERNON	GENOA DAM 8	43.57	-30	4	32	2	-20.6	3.7	52.3	4.2	-30	51.4	-20.2	48.9	58 -22	52 -34	52 -22	64 -28	58 -40	58 -34
WASHINGTON	GERMANTOWN	43.22	-28	4	32	2	-19.2	3.7	52.3	4.2	-28	51.5	-18.7	48.9	58 -22	52 -28	52 -22	64 -28	58 -40	58 -28
MARINETTE	GOODMAN	45.62	-31	3	29	2	-21.3	3.1	48.2	4.2	-31	47.9	-21.6	46.0	52 -22	52 -34	52 -22	58 -28	52 -40	52 -28
DOUGLAS	GORDON	46.25	-39	3	31	2	-26.8	3.1	50.9	4.2	-39	49.6	-27.6	47.4	52 -28	52 -40	52 -28	64 -34	58 -46	52 -34
BURNETT	GRANTSBURG	45.78	-36	3	31	2	-24.7	3.1	50.9	4.2	-36	49.7	-25.2	47.5	52 -28	52 -40	52 -28	64 -34	58 -46	52 -34
BROWN	GREEN BAY WSO AP	44.48	-28	3	31	2	-19.2	3.1	50.9	4.2	-28	50.2	-19.1	47.9	52 -22	52 -28	52 -22	64 -28	58 -34	52 -28
IRON	GURNEY	46.47	-32	3	30	2	-22.0	3.1	49.5	4.2	-32	48.6	-22.6	46.6	52 -22	52 -34	52 -28	58 -34	58 -40	52 -34

Table 3.12 UW, SHRP, and LTPP Pavement Temperatures and PG Grades for Wisconsin Weather Stations (Continued)

COUNTY ID	WEATHER STATION	LAT	AIR TEMPERATURE LOW AVG	AIR TEMPERATURE LOW STD	AIR TEMPERATURE HIGH AVG	AIR TEMPERATURE HIGH STD	UW PAVEMENT TEMP. LOW AVG	UW PAVEMENT TEMP. LOW STD	UW PAVEMENT TEMP. HIGH AVG	UW PAVEMENT TEMP. HIGH STD	PAVEMENT TEMP. SHRP LOW	PAVEMENT TEMP. SHRP HIGH	PAVEMENT TEMP. LTPP LOW	PAVEMENT TEMP. LTPP HIGH	PG GRADE @ 50% REL. UW HI LO	PG GRADE @ 50% REL. SHRP HI LO	PG GRADE @ 50% REL. LTPP HI LO	PG GRADE @ 98% REL. UW HI LO	PG GRADE @ 98% REL. SHRP HI LO	PG GRADE @ 98% REL. LTPP HI LO
WAUSHARA	HANCOCK EXP FARM	44.12	-33	3	33	2	-22.6	3.1	53.6	4.2	-33	52.2	-22.5	49.5	58 -28	58 -34	52 -28	64 -34	58 -40	58 -34
WASHINGTON	HARTFORD 2 W	43.32	-29	4	32	2	-19.9	3.7	52.3	4.2	-29	51.5	-19.4	48.9	58 -22	52 -34	52 -22	64 -28	58 -40	58 -28
JACKSON	HATFIELD HYDRO PLANT	44.40	-36	4	33	2	-24.7	3.7	53.6	4.2	-36	52.1	-24.8	49.4	58 -28	58 -40	52 -28	64 -34	58 -46	58 -34
VERNON	HILLSBORO	43.65	-33	4	32	1	-22.6	3.7	52.3	3.0	-33	51.4	-22.4	48.8	58 -28	52 -34	52 -28	64 -34	58 -46	52 -34
CHIPPEWA	HOLCOMBE	45.22	-35	4	31	2	-24.0	3.7	50.9	4.2	-35	49.9	-24.3	47.7	52 -28	52 -40	52 -28	64 -34	58 -46	52 -34
ROCK	JANESVILLE	42.67	-26	3	33	2	-17.8	3.1	53.6	4.2	-26	52.6	-17.1	49.8	58 -22	58 -28	52 -22	64 -28	58 -34	58 -28
TAYLOR	JUMP RIVER 3 E	45.37	-37	4	30	2	-25.4	3.7	49.5	4.2	-37	48.9	-25.8	46.9	52 -28	52 -40	52 -28	58 -34	58 -46	52 -34
KENOSHA	KENOSHA	42.55	-25	4	31	2	-17.1	3.7	50.9	4.2	-25	50.7	-16.3	48.3	52 -22	52 -28	52 -22	64 -28	58 -34	58 -28
KENAUWEE	KENAUWEE 5 S	44.43	-27	4	29	2	-18.5	3.7	48.2	4.2	-27	48.3	-18.3	46.3	52 -22	52 -28	52 -22	58 -28	58 -40	52 -28
LA CROSSE	LA CROSSE FAA AP	43.87	-30	4	33	2	-20.6	3.7	53.6	4.2	-30	52.2	-20.3	49.6	58 -22	58 -34	52 -22	64 -28	58 -40	58 -34
RUSK	LADYSMITH	45.47	-33	4	30	1	-22.6	3.7	49.5	3.0	-33	48.9	-23.0	46.8	52 -28	52 -34	52 -28	58 -34	52 -46	52 -34
WALWORTH	LAKE GENEVA	42.60	-26	3	33	2	-17.8	3.1	53.6	4.2	-26	52.6	-17.0	49.9	58 -22	58 -28	52 -22	64 -28	58 -34	58 -28
JEFFERSON	LAKE MILLS	43.07	-28	3	32	2	-19.2	3.1	52.3	4.2	-28	51.5	-18.6	49.0	58 -22	52 -28	52 -22	64 -28	58 -34	58 -28
GRANT	LANCASTER 4 WSW	42.83	-28	3	32	2	-19.2	3.1	52.3	4.2	-28	51.6	-18.5	49.0	58 -22	52 -28	52 -22	64 -28	58 -34	58 -28
FOREST	LAONA 6 SW	45.52	-32	4	28	2	-22.0	3.7	46.8	4.2	-32	47.0	-22.3	45.3	52 -22	52 -34	46 -28	58 -34	52 -40	52 -34
SAUK	LONE ROCK FAA AP	43.20	-32	6	32	2	-22.0	5.0	52.3	4.2	-32	51.5	-21.5	48.9	58 -22	52 -34	52 -22	64 -34	58 -46	58 -34
ONEIDA	LONG LAKE DAM	45.90	-26	3	29	2	-17.8	3.1	48.2	4.2	-26	47.8	-18.1	45.9	52 -22	52 -28	46 -22	58 -28	52 -34	52 -28
ASHLAND	MADELINE ISLAND	46.83	-29	4	28	2	-19.9	3.7	46.8	4.2	-29	46.5	-20.6	44.9	52 -22	52 -34	46 -22	58 -28	52 -40	52 -34
DANE	MADISON WSO AP	43.13	-28	4	32	2	-19.2	3.7	52.3	4.2	-28	51.5	-18.6	49.0	58 -22	52 -28	52 -22	64 -28	58 -40	58 -28
	MADISON WB CITY	43.08	-26	3	32	2	-17.8	3.1	52.3	4.2	-26	51.5	-17.2	49.0	58 -22	52 -28	52 -22	64 -28	58 -34	58 -28
MANITOWOC	MANITOWOC	44.10	-29	3	30	2	-19.9	3.1	49.5	4.2	-29	49.3	-19.7	47.2	52 -22	52 -34	52 -22	58 -28	58 -40	52 -28
MARINETTE	MARINETTE	45.10	-27	3	32	2	-18.5	3.1	52.3	4.2	-27	50.9	-18.6	48.5	58 -22	52 -28	52 -22	64 -28	58 -34	58 -28
WOOD	MARSHFIELD EXP FARM	44.65	-32	3	31	2	-22.0	3.1	50.9	4.2	-32	50.1	-22.0	47.8	52 -22	52 -34	52 -28	64 -34	58 -40	52 -28
JACKSON	MATHER 3 NW	44.18	-32	4	32	2	-22.0	3.7	52.3	4.2	-32	51.2	-21.8	48.7	58 -22	52 -34	52 -22	64 -34	58 -40	58 -34
JUNEAU	MAUSTON 1 SE	43.78	-30	6	32	2	-20.6	5.0	52.3	4.2	-30	51.3	-20.3	48.8	58 -22	52 -34	52 -22	64 -34	58 -46	58 -34
TAYLOR	MEDFORD	45.13	-33	3	29	2	-22.6	3.1	48.2	4.2	-33	48.0	-22.9	46.1	52 -28	52 -34	52 -28	58 -34	52 -40	52 -34
ASHLAND	MELLEN 4 NE	46.43	-36	4	30	2	-24.7	3.7	49.5	4.2	-36	48.6	-25.5	46.6	52 -28	52 -40	52 -28	58 -34	58 -46	52 -34
DUNN	MENOMONIE	44.88	-32	3	33	2	-22.0	3.1	53.6	4.2	-32	51.9	-22.1	49.3	58 -22	52 -34	52 -28	64 -34	58 -40	58 -28
LINCOLN	MERRILL	45.18	-33	4	31	2	-22.6	3.7	50.9	4.2	-33	49.9	-22.9	47.7	52 -28	52 -34	52 -28	64 -34	58 -46	52 -34
MILWAUKEE	MILWAUKEE MT MARY COL	43.07	-26	3	32	2	-17.8	3.1	52.3	4.2	-26	51.5	-17.2	49.0	58 -22	52 -28	52 -22	64 -28	58 -34	58 -28
MILWAUKEE	MILWAUKEE WSO AP	42.95	-25	4	31	2	-17.1	3.7	50.9	4.2	-25	50.6	-16.4	48.2	52 -22	52 -28	52 -22	64 -28	58 -34	58 -28
ONEIDA	MINOQUA DAM	45.88	-36	4	30	2	-24.7	3.7	49.5	4.2	-36	48.8	-25.3	46.7	52 -28	52 -40	52 -28	58 -34	58 -46	52 -34
WASHBURN	MINONG 5 WSW	46.08	-38	6	31	2	-26.1	5.0	50.9	4.2	-38	49.6	-26.8	47.5	52 -28	52 -40	52 -28	64 -40	58 -52	52 -40
BUFFALO	MONDOVI	44.57	-33	4	32	2	-22.6	3.7	52.3	4.2	-33	51.1	-22.7	48.6	58 -28	52 -34	52 -28	64 -34	58 -46	58 -34
MARQUETTE	MONTELLO	43.78	-29	4	32	2	-19.9	3.7	52.3	4.2	-29	51.3	-19.6	48.8	58 -22	52 -34	52 -22	64 -28	58 -40	58 -28
JUNEAU	NECEDAH	44.03	-34	4	32	2	-23.3	3.7	52.3	4.2	-34	51.2	-23.2	48.7	58 -28	52 -34	52 -28	64 -34	58 -46	58 -34
CLARK	NEILLSVILLE 3 SW	44.53	-34	4	31	2	-23.3	3.7	50.9	4.2	-34	50.1	-23.4	47.8	52 -28	52 -34	52 -28	64 -34	58 -46	52 -34
FOREST	NEWALD 4 N	45.78	-35	4	29	2	-24.0	3.7	48.2	4.2	-35	47.8	-24.5	46.0	52 -28	52 -40	46 -28	58 -34	52 -46	52 -34
WAUPACA	NEW LONDON	44.38	-30	3	32	2	-20.6	3.1	52.3	4.2	-30	51.1	-20.5	48.7	58 -22	52 -34	52 -22	64 -28	58 -40	58 -28
ONEIDA	NORTH PELICAN	45.63	-34	4	28	2	-23.3	3.7	46.8	4.2	-34	46.9	-23.8	45.2	52 -28	52 -34	46 -28	58 -34	52 -46	52 -34
WAUKESHA	OCONOMOWOC	43.10	-27	4	32	2	-18.5	3.7	52.3	4.2	-27	51.5	-17.9	49.0	58 -22	52 -28	52 -22	64 -28	58 -40	58 -28
OCONTO	OCONTO 4 W	44.90	-28	4	31	2	-19.2	3.7	50.9	4.2	-28	50.0	-19.2	47.8	52 -22	52 -28	52 -22	64 -28	58 -40	52 -28
WINNEBAGO	OSHKOSH	44.03	-28	3	31	2	-19.2	3.1	50.9	4.2	-28	50.3	-18.9	48.0	52 -22	52 -28	52 -22	64 -28	58 -34	52 -28
CLARK	OWEN	44.95	-34	3	30	2	-23.3	3.1	49.5	4.2	-34	49.1	-23.5	47.0	52 -28	52 -34	52 -28	58 -34	58 -40	52 -34
PRICE	PARK FALLS	45.93	-33	3	29	2	-22.6	3.1	48.2	4.2	-33	47.8	-23.1	45.9	52 -28	52 -34	46 -28	58 -34	52 -40	52 -34
WAUSHARA	PINE RIVER 3 NE	44.18	-29	3	32	2	-19.9	3.1	52.3	4.2	-29	51.2	-19.7	48.7	58 -22	52 -34	52 -22	64 -28	58 -40	58 -28

Table 3.12 UW, SHRP, and LTPP Pavement Temperatures and PG Grades for Wisconsin Weather Stations (Continued)

COUNTY ID	WEATHER STATION	LAT	AIR TEMPERATURE				UW PAVEMENT TEMP.				PAVEMENT TEMP.				PG GRADE @ 50% REL.			PG GRADE @ 98% REL.		
			LOW		HIGH		LOW		HIGH		SHRP		LTPP		UW	SHRP	LTPP	UW	SHRP	LTPP
			AVG	STD	AVG	STD	AVG	STD	AVG	STD	LOW	HIGH	LOW	HIGH	HI LO	HI LO	HI LO	HI LO	HI LO	HI LO
WOOD	PITTSVILLE	44.43	-33	4	31	1	-22.6	3.7	50.9	3.0	-33	50.2	-22.6	47.9	52 -28	52 -34	52 -28	58 -34	58 -46	52 -34
GRANT	PLATTEVILLE	42.75	-28	3	32	2	-19.2	3.1	52.3	4.2	-28	51.6	-18.5	49.0	58 -22	52 -28	52 -22	64 -28	58 -34	58 -28
COLUMBIA	PORTAGE	43.52	-29	3	32	2	-19.9	3.1	52.3	4.2	-29	51.4	-19.5	48.9	58 -22	52 -34	52 -22	64 -28	58 -40	58 -28
OZAUKEE	PORT WASHINGTON	43.38	-26	3	29	2	-17.8	3.1	48.2	4.2	-26	48.6	-17.3	46.6	52 -22	52 -28	52 -22	58 -28	58 -34	52 -28
BAYFIELD	PORT WING 3 E	46.77	-31	4	29	2	-21.3	3.7	48.2	4.2	-31	47.5	-22.0	45.7	52 -22	52 -34	46 -28	58 -34	52 -40	52 -34
CRAWFORD	PRAIRIE DU CHIEN	43.03	-29	4	34	2	-19.9	3.7	55.0	4.2	-29	53.5	-19.3	50.5	58 -22	58 -34	52 -22	64 -28	58 -40	58 -28
SAUK	PRAIRIE DU SAC 2 N	43.32	-28	5	32	2	-19.2	4.4	52.3	4.2	-28	51.5	-18.7	48.9	58 -22	52 -28	52 -22	64 -28	58 -40	58 -34
PRICE	PRENTICE 2	45.52	-37	4	29	2	-25.4	3.7	48.2	4.2	-37	47.9	-25.9	46.0	52 -28	52 -40	52 -28	58 -34	52 -46	52 -34
RACINE	RACINE	42.70	-25	4	31	2	-17.1	3.7	50.9	4.2	-25	50.7	-16.4	48.3	52 -22	52 -28	52 -22	64 -28	58 -34	58 -28
ONEIDA	RAINBOW RESERVOIR	45.83	-34	4	29	2	-23.3	3.7	48.2	4.2	-34	47.8	-23.8	46.0	52 -28	52 -34	46 -28	58 -34	52 -46	52 -34
SAUK	REEDSBURG	43.53	-31	4	32	2	-21.3	3.7	52.3	4.2	-31	51.4	-20.9	48.9	58 -22	52 -34	52 -22	64 -34	58 -40	58 -34
VILAS	REST LAKE	46.13	-35	3	29	2	-24.0	3.1	48.2	4.2	-35	47.7	-24.6	45.9	52 -28	52 -40	46 -28	58 -34	52 -46	52 -34
ONEIDA	RHINELANDER	45.63	-33	3	30	2	-22.6	3.1	49.5	4.2	-33	48.8	-23.0	46.8	52 -28	52 -34	52 -28	58 -34	58 -40	52 -34
BARRON	RICE LAKE	45.50	-35	4	31	2	-24.0	3.7	50.9	4.2	-35	49.8	-24.4	47.6	52 -28	52 -40	52 -28	64 -34	58 -46	52 -34
RICHLAND	RICHLAND CENTER	43.33	-31	4	33	2	-21.3	3.7	53.6	4.2	-31	52.4	-20.9	49.7	58 -22	58 -34	52 -22	64 -34	58 -40	58 -34
BARRON	RIDGELAND 1 NNE	45.22	-36	4	31	2	-24.7	3.7	50.9	4.2	-36	49.9	-25.1	47.7	52 -28	52 -40	52 -28	64 -34	58 -46	52 -34
PIERCE	RIVER FALLS	44.87	-33	3	32	2	-22.6	3.1	52.3	4.2	-33	51.0	-22.8	48.5	58 -28	52 -34	52 -28	64 -34	58 -40	58 -34
MARATHON	ROSHOLT 9 BBE	44.77	-32	4	31	2	-22.0	3.7	50.9	4.2	-32	50.1	-22.0	47.8	52 -22	52 -34	52 -28	64 -34	58 -40	52 -34
POLK	ST CROIX FALLS	45.42	-35	3	32	2	-24.0	3.1	52.3	4.2	-35	50.8	-24.4	48.4	58 -28	52 -40	52 -28	64 -34	58 -46	58 -34
SHAWANO	SHAWANO	44.77	-30	4	32	2	-20.6	3.7	52.3	4.2	-30	51.0	-20.6	48.6	58 -22	52 -34	52 -22	64 -28	58 -40	58 -34
SHEBOYGAN	SHEBOYGAN	43.75	-25	3	31	2	-17.1	3.1	50.9	4.2	-25	50.4	-16.7	48.0	52 -22	52 -28	52 -22	64 -28	58 -34	52 -28
DOUGLAS	SOLON SPRINGS	46.35	-37	4	31	2	-25.4	3.7	50.9	4.2	-37	49.6	-26.2	47.4	52 -28	52 -40	52 -28	64 -34	58 -46	52 -34
MONROE	SPARTA	43.93	-33	4	32	2	-22.6	3.7	52.3	4.2	-33	51.3	-22.5	48.8	58 -28	52 -34	52 -28	64 -34	58 -46	58 -34
WASHBURN	SPOONER EXP FARM	45.82	-36	3	32	2	-24.7	3.1	52.3	4.2	-36	50.7	-25.3	48.3	58 -28	52 -40	52 -28	64 -34	58 -46	58 -34
CHIPPEWA	STANLEY	44.97	-33	4	31	2	-22.6	3.7	50.9	4.2	-33	50.0	-22.8	47.7	52 -28	52 -34	52 -28	64 -34	58 -46	52 -34
PORTAGE	STEVENS POINT	44.50	-31	3	31	2	-21.3	3.1	50.9	4.2	-31	50.1	-21.2	47.8	52 -22	52 -34	52 -22	64 -28	58 -40	52 -28
DANE	STOUGHTON	42.92	-27	4	31	2	-18.5	3.7	50.9	4.2	-27	50.6	-17.9	48.2	52 -22	52 -28	52 -22	64 -28	58 -40	58 -28
DOOR	STURGEON BAY	44.87	-27	3	30	2	-18.5	3.1	49.5	4.2	-27	49.1	-18.5	47.0	52 -22	52 -28	52 -22	58 -28	58 -34	52 -28
DOUGLAS	SUPERIOR	43.40	-33	3	29	2	-22.6	3.1	48.2	4.2	-33	48.6	-22.3	46.6	52 -28	52 -34	52 -28	58 -34	58 -40	52 -34
LINCOLN	TOMAHAWK SPIRIT RES	45.43	-35	4	29	2	-24.0	3.7	48.2	4.2	-35	47.9	-24.4	46.1	52 -28	52 -40	52 -28	58 -34	52 -46	52 -34
TREMPEALEAU	TREMPEALEAU DAM 6	44.00	-31	7	32	1	-21.3	5.7	52.3	3.0	-31	51.3	-21.1	48.8	58 -22	52 -34	52 -22	64 -34	58 -46	52 -40
MANITOWOC	TWO RIVERS	44.15	-26	3	28	2	-17.8	3.1	46.8	4.2	-26	47.4	-17.5	45.6	52 -22	52 -28	46 -22	58 -28	52 -34	52 -28
VERNON	VIROQUA 2 NW	43.57	-34	4	32	2	-23.3	3.7	52.3	4.2	-34	51.4	-23.1	48.9	58 -28	52 -34	52 -28	64 -34	58 -46	58 -34
DOOR	WASHINGTON ISLAND	43.57	-25	4	28	2	-17.1	3.7	46.8	4.2	-25	47.6	-16.6	45.7	52 -22	52 -28	46 -22	58 -28	52 -34	52 -28
JEFFERSON	WATERTOWN	43.18	-27	4	33	2	-18.5	3.7	53.6	4.2	-27	52.5	-17.9	49.7	58 -22	58 -28	52 -22	64 -28	58 -40	58 -28
WAUKESHA	WAUKESHA	43.02	-25	4	32	2	-17.1	3.7	52.3	4.2	-25	51.5	-16.5	49.0	58 -22	52 -28	52 -22	64 -28	58 -34	58 -28
WAUPACA	WAUPACA	44.35	-29	3	32	2	-19.9	3.1	52.3	4.2	-29	51.1	-19.8	48.7	58 -22	52 -34	52 -22	64 -28	58 -40	58 -28
MARATHON	WAUSAU FAA AP	44.92	-31	3	31	2	-21.3	3.1	50.9	4.2	-31	50.0	-21.4	47.7	52 -22	52 -34	52 -22	64 -28	58 -40	52 -28
MILWAUKEE	WEST ALLIS	43.02	-24	3	32	2	-16.4	3.1	52.3	4.2	-24	51.5	-15.7	49.0	58 -22	52 -28	52 -16	64 -28	58 -34	58 -22
WASHINGTON	WEST BEND	43.40	-27	4	32	2	-18.5	3.7	52.3	4.2	-27	51.4	-18.0	48.9	58 -22	52 -28	52 -22	64 -28	58 -40	58 -28
RUSK	WEYERHAUSER	45.42	-34	3	31	2	-23.3	3.1	50.9	4.2	-34	49.9	-23.7	47.6	52 -28	52 -34	52 -28	64 -34	58 -40	52 -34
WALWORTH	WHITEWATER	42.85	-27	4	33	2	-18.5	3.7	53.6	4.2	-27	52.5	-17.8	49.8	58 -22	58 -28	52 -22	64 -28	58 -40	58 -28
ONEIDA	WILLOW RESERVOIR	45.72	-36	3	29	1	-24.7	3.1	48.2	3.0	-36	47.9	-25.2	46.0	52 -28	52 -40	46 -28	58 -34	52 -46	52 -34
SAWYER	WINTER 6 NNW	45.88	-35	6	29	1	-24.0	5.0	48.2	3.0	-35	47.8	-24.6	45.9	52 -28	52 -40	46 -28	58 -34	52 -52	52 -40
WOOD	WISCONSIN RAPIDS	44.38	-31	4	30	2	-21.3	3.7	49.5	4.2	-31	49.2	-21.2	47.1	52 -22	52 -34	52 -22	58 -34	58 -40	52 -34

3.3 Other Pavement Temperature Characteristics

Several plots are presented in this section to show other important pavement temperature characteristics. Profiles of the temperature difference between surface and bottom layer, the temperature difference between different probes, and the effect of different locations on the temperature measurements as a function of time are presented. Also, one unusual pavement temperature profile (observed during Winter 1996) is included.

3.3.1 Temperature Difference between Surface Layer and Bottom Layer

The typical graph is shown in Figure 3.13. During the night time, the surface layer experienced a colder temperature than the bottom layer. This pattern is reversed during the day time. Also, it is noticed that during day time, the difference is mostly higher than during night time due to the effect of solar radiation. The magnitude of this difference is dependent on the intensity of the solar radiation during that typical day.

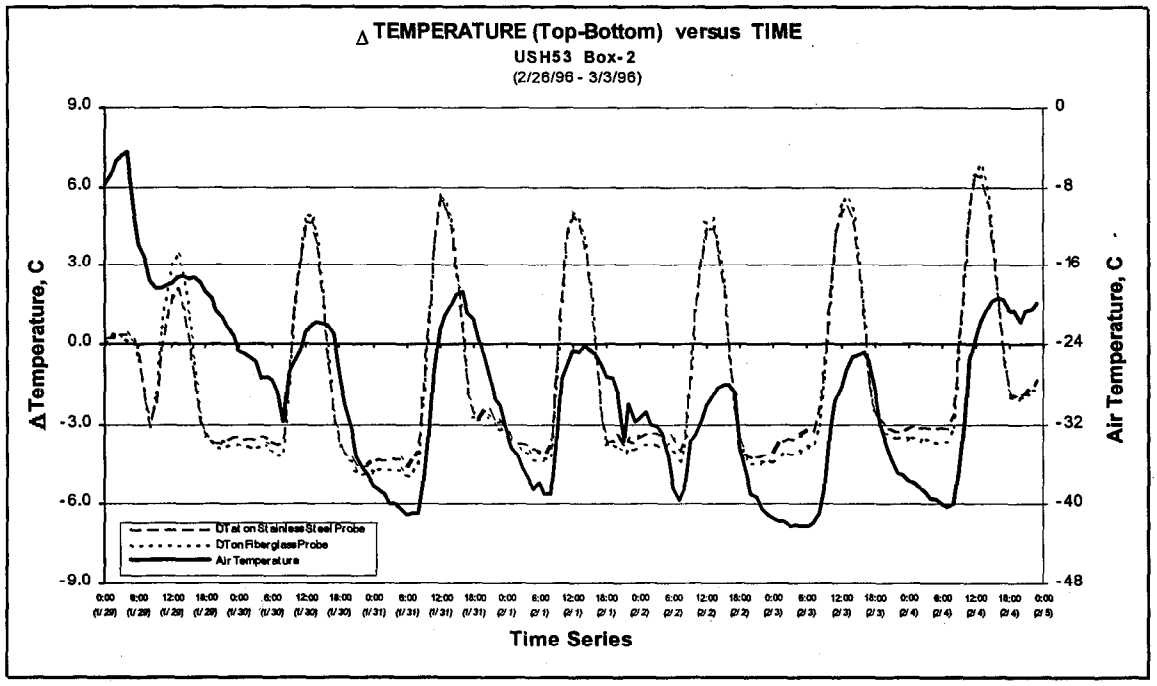

Figure 3.14 Temperature Difference between Surface and Bottom Layer at Box-2

3.3.2 *Temperature Difference between Stainless Steel and Fiberglass Probe*

Figure 3.14 shows the typical pattern of temperature difference between stainless steel and fiberglass probe for seven consecutive days. In general, the stainless steel probe showed higher temperature readings (at all depths) than the fiberglass during day time. The difference ranged between 0^{o} C and 0.75^{o} C. During nighttime, the pattern was reversed with the same level of difference. This pattern is caused by the different probes conductivity characteristics. During a day, air temperature rises and the stainless steel probe will adjust and increase the temperature more rapidly than the fiberglass due to its higher conductivity. During the night, the air temperature drops. A material with high conductivity will tend to release the heat more rapidly. This explains why during a night, stainless steel probe will show a lower temperature reading than fiberglass, particularly near the pavement surface.

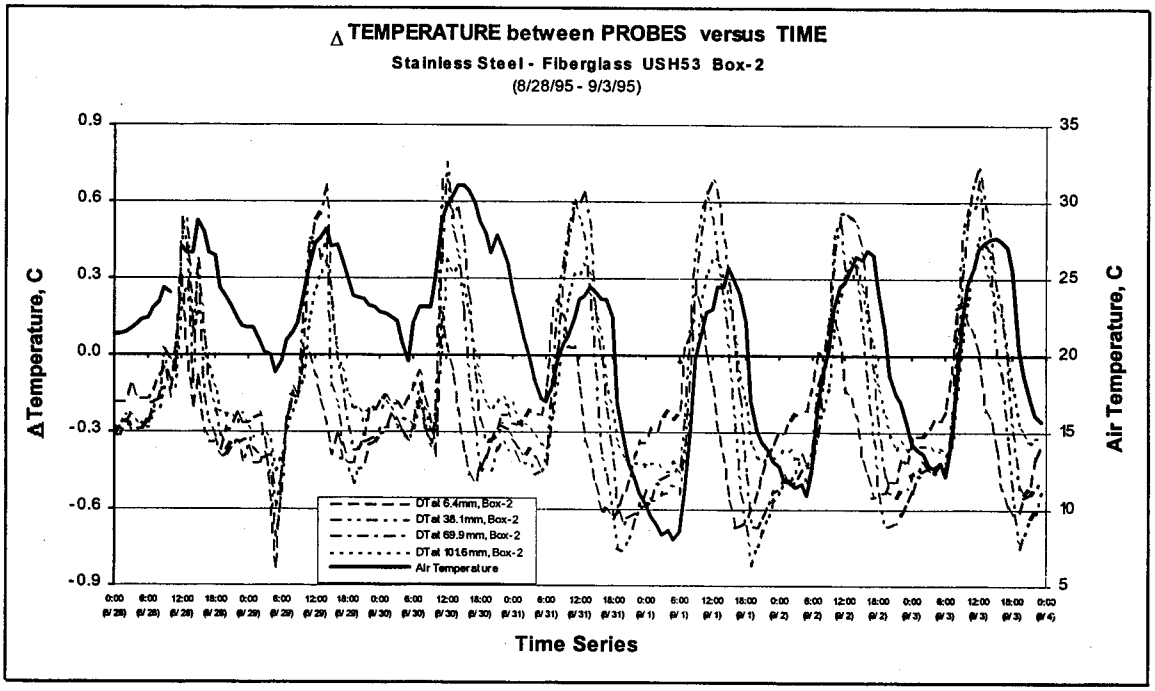

Figure 3.15 Temperature Difference between Stainless Steel and Fiberglass Probe

3.3.3 *Temperature Differences between Boxes on Each Probe*

The typical pattern of the temperature difference between two boxes on stainless steel and fiberglass probes is shown in Figure 3.15. It appears that there is not a significant pattern

that can be related to any single factor. Experimental errors involved in such type of measurements can cause these differences. After a careful evaluation, it was concluded that these differences are not expected to have a significant impact on the analysis and the magnitude of the differences does not warrant any further evaluation.

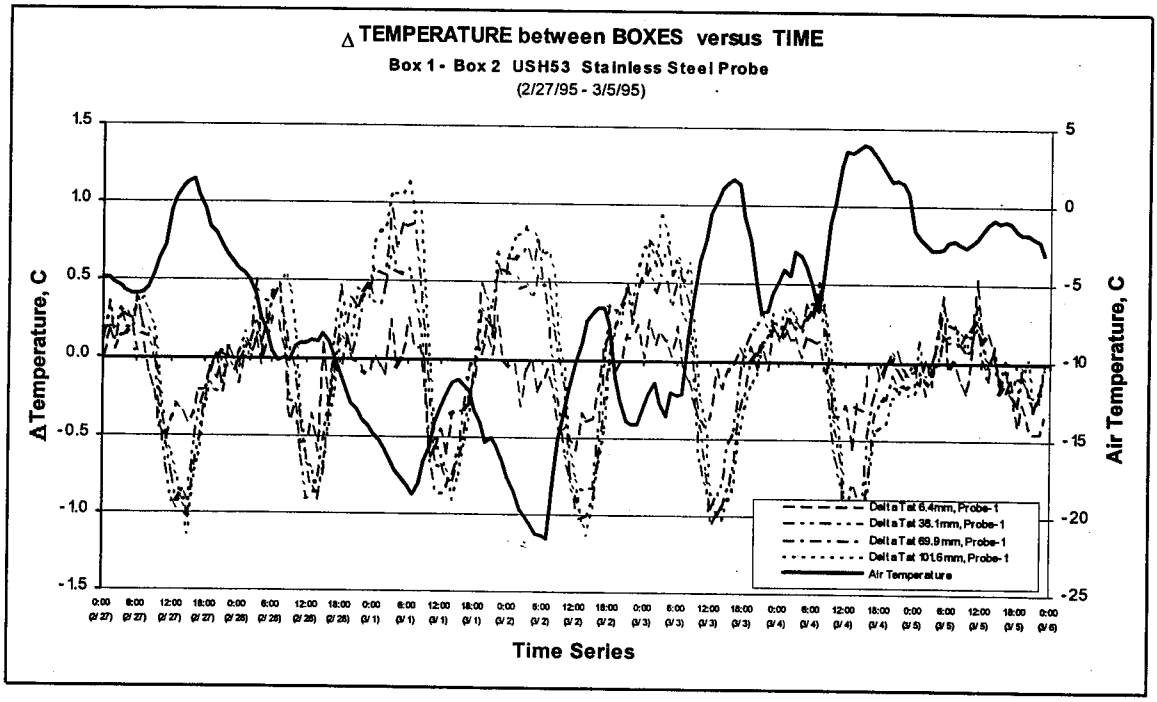

Figure 3.16 Temperature Difference between Boxes on Fiberglass Probe

3.3.4 *Unusual Temperature Profile during the Winter of 1996*

An unusual pavement temperature profile occurred on three consecutive days starting from January 19th to 21st, 1996 (Figure 3.116). As shown, a large difference in pavement temperature measurement between the stainless steel and the fiberglass probe were observed. Such differences were observed at all pavement depths. The fiberglass probe showed a lower temperature than the stainless steel, particularly at noontime (Figure 3.16). The magnitude of the differences reached 6.7°C on January 19th, 1996 and gradually decreased on the two following days and returned to normal on January 22, 1996. The pavement surface layer experienced the biggest difference and the bottom experienced the lowest. However, the

lowest differences experienced by the bottom layer were still greater than the normal differences (Figure 3.14).

The thermal history of the pavement during this period was analyzed. It appears that the solar radiation intensity was very low for the three consecutive days preceding the day when this phenomenon started (Figure 3.17) Also, the continuous drop of air temperature, approximate 30°C in 24 hours, might have contributed to the observed differences.

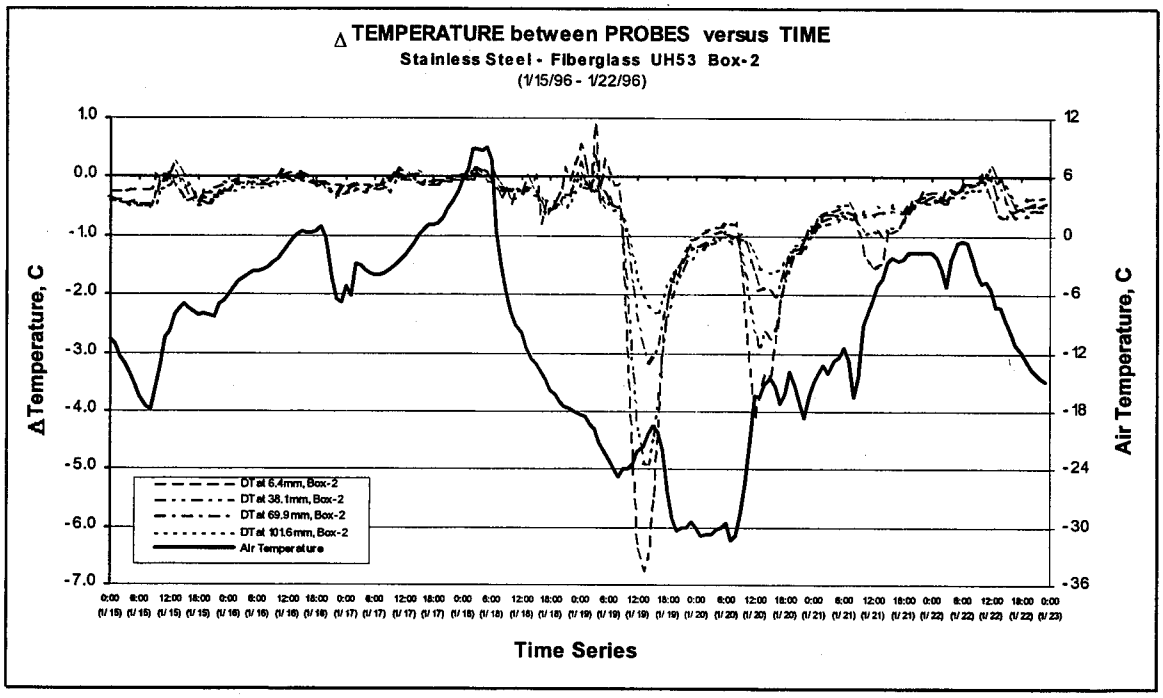

Figure 3.17 Unusual Pavement Temperature Difference (Winter 1996)

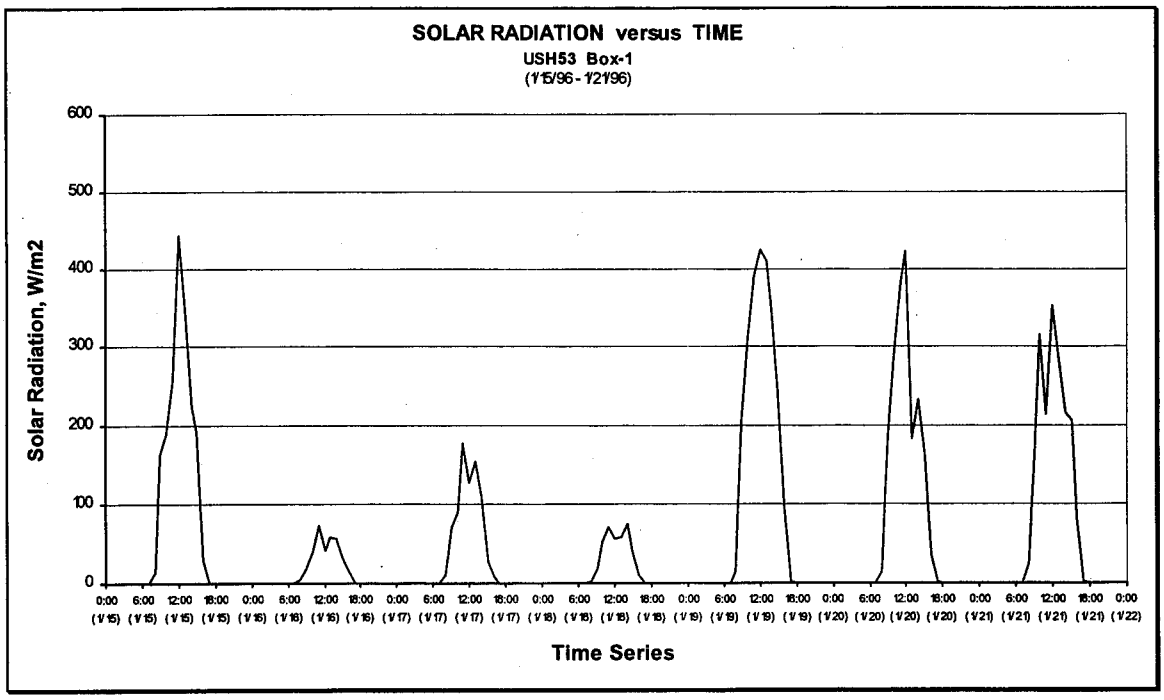

Figure 3.18 Solar Radiation during the Unusual Pavement Temperature Difference Period

The authors hypothesize that this phenomenon might be explained by the different conductivity of the probes. When the two factors, low solar radiation intensity and continuous drop of air temperature, took place at the same time, the pavement temperature continued decreasing as the air temperature decreased. The probe with a lower conductivity material could not adapt to the temperature change as quickly as the probe with higher conductivity material. This may explain why the fiberglass probe showed the higher temperature than the stainless steel probe. When the change of air temperature was relatively small and the solar radiation was high, the difference became smaller and eventually the difference returned to normal three days later.

There is no other similar set of data that could be observed to test this hypothesis. Neither a low solar radiation intensity alone nor a continuous drop of temperature alone had a significant effect on the difference between the two probes. The data collected during the first 22 months did not show this phenomenon at any other time.

CHAPTER FOUR
VALIDATION OF SUPERPAVE BINDER SPECIFICATION CRITERIA

4.1 Introduction

The validation process was done by evaluating the pavement performance from each test section and comparing the properties of the binder used in construction of the sections. The field performance was evaluated by a field crack count survey of the test sections. The number and severity of cracks were recorded for each test section and the results were correlated to determine if there is a difference in performance of the test sections. The binders used in these sections were tested to determine the properties used in the Superpave™ Binder Specifications.

4.2 Crack Count Survey

A crack count survey was performed on October 1996 on all test sections. Cracks are divided into five severity indexes where index 1 represents a hairline crack and 5 represents a wide crack. The results of the survey are summarized and presented in Figure 5.1. The index shown in Figure 4.1 is the average of total cracking indices calculated per 30.48 meter of each test section. The average is calculated by adding all cracking indices measured in the particular test section and the total index is then divided by the total length of the test section. Separate average cracking indices were calculated for the left and the right lane.

The survey results show that all test sections exhibited cracking. The survey shows that the left lanes have more severe cracks than the right lanes for all test sections except test Section 5. The survey was conducted by randomly moving along from the left to the right lane to avoid any bias in crack observations. However, no explanation could be offered for these differences except the possibility of paving sequence. It appears that the left lane was completed during one period of time and the right lane was constructed during a different period.

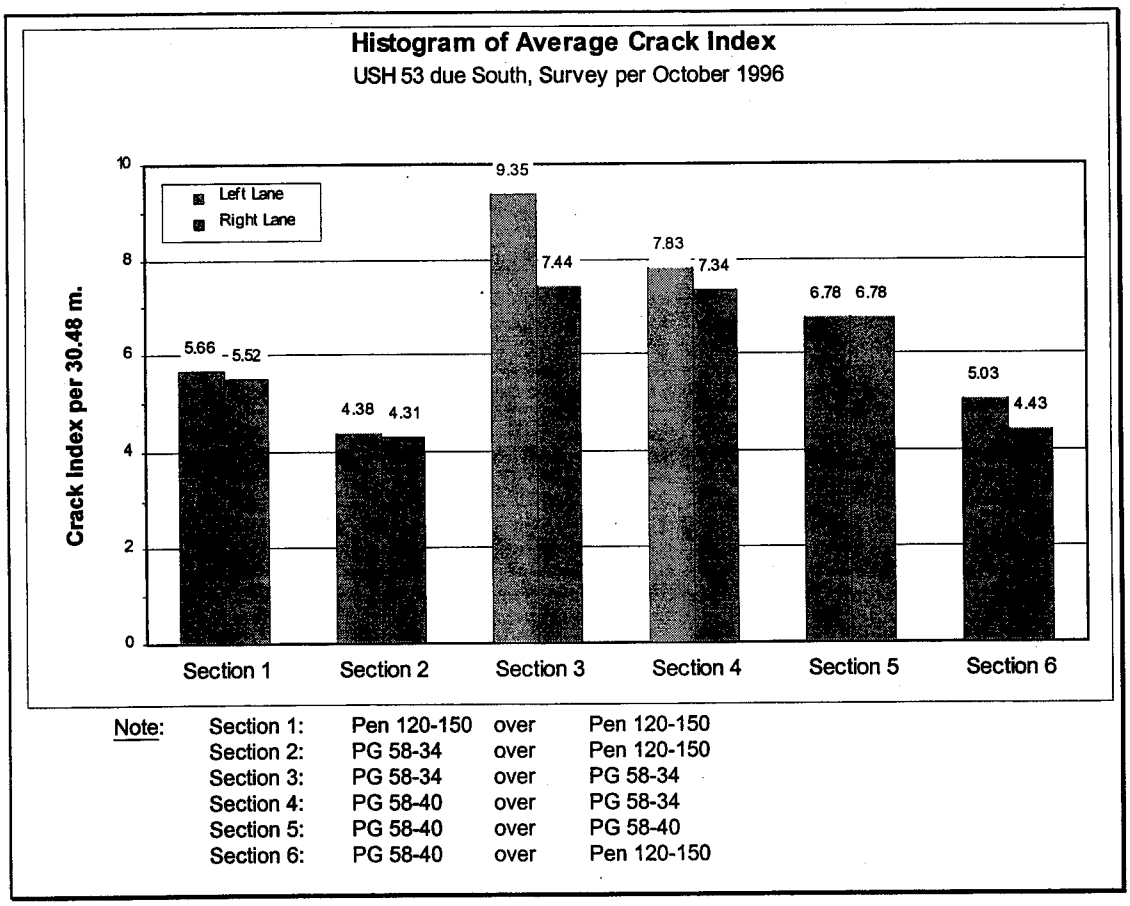

Figure 4.1 Crack Count Survey Summary of USH 53 per October 1996

Site investigation indicated that a large number of cracks are spaced 6.1 meters apart, which corresponds to the distance of PCC pavement joints underneath the asphalt concrete pavement layer. The analysis suggested strongly that reflective cracking has occurred on these sections.

Given the fact that all test sections are subjected to the same weather and traffic load condition, the variation of crack severity on each test section indicates that there are differences in performance of the test sections. The differences can be related to the different response of the binders to the weather conditions.

Figure 4.1 shows that Section 3 is sustained from the most severe cracks, 9.35 per 30.48 m of distance. However, this only occurred on the left lane of the section. The right lane appears to have almost the same index as Section 4 and Section 5. These sections were

built using a PG graded modified asphalt binder for both surface and binder layer. Section 2 and Section 6 appear to have the lowest average crack index, approximately 4.35 per 30.48 m Sections 2 and 6 used the same asphalt binder for the binder layer and different modified binders for the surface layer.

The assumption made in the analysis was that since this was a crack and seat project, the pre-existing conditions can be assumed to be equivalent for all sections. This assumption was questioned however because of the significant differences in performance. The results of the pre-construction survey conducted by WisDOT prior to the break and seat operations are shown in Figure 4.2. The same concept of cracking index was used to quantify the surface condition of the jointed concrete pavement. A value of 1 or 2 cracking level was given to any crack between joints, to any severe deterioration of joints, and to all longitudinal cracks observed. The joints were not considered as cracks and thus the cracking indices were not as high as the indices shown in Figure 4.1. The results in Figure 2 were also normalized to account for the shorter section that were surveyed. The survey included only 152.4 m of each section. As shown in the figure, there were significant differences between the existing conditions prior to overlaying the sections. The relative change is shown in Figure 4.3 for all sections.

The difference in cracking indices show a different ranking compared to the post construction ranking. The differences show that sections 1, 3, and 4 share the highest average cracking index. Sections 5 and 6 show the minimum cracking indices. Although the ranking has changed by taking into account the pre-construction conditions, there are still some trends that are hard to explain. For example, sections 3 and 4, which were built with PG 58-34 and PG 58-40 for both layers still show the worst rankings. It is evident that the relation between binder types and severity of cracking are not obvious and therefore a more elaborate analysis was undertaken.

4.3 Binder Testing Procedure

The evaluation of the asphalt binders included testing of the binder from each test sections as follows:

- Dynamic Shear Rheometer (AASHTO TP5) @ 52 °C, 58 °C, and 64°C.
  Parameter evaluated: Complex Shear Modulus and Phase angle.
- Bending Beam Rheometer (AASHTO TP1) @ -18 °C, -24 °C, and -30°C.
  Parameters evaluated: Creep Stiffness and m-value.
- Direct Tension Tester (AASHTO TP3) @ -18 °C, -24 °C, and -30°C.
  Parameter evaluated: Failure Strain.

The testing was done for the unaged binder, after aging with the Rolling Thin Film Oven (RTFO) procedure, and after aging with the Pressure Aging Vessel (PAV) procedure.

4.4 Data Analysis

The results of testing are presented in Appendix C. Since the observed distress was reflective cracking, the analysis focused on the test results from the Bending Beam Rheometer (BBR) and the Direct Tension Test (DTT). The binder properties, including S(60), m(60), and ε_f, were correlated to the pavement performance, represented by the average cracking index, as shown in Figures 4.2 and 4.3. Because each pavement section included a surface course and a binder course, the values of the two binders were added and the total was used for each section in figure 4.2. In Figure 4.3 the binder properties were represented by a total property index of each section. The index is calculated by dividing each property measured by its limit in the specification and adding the normalized properties for both layers. Figure 4.3 (a) shows the relationship at each temperature. Figure 4.3 (b) shows the relationships for the 3 temperatures combined.

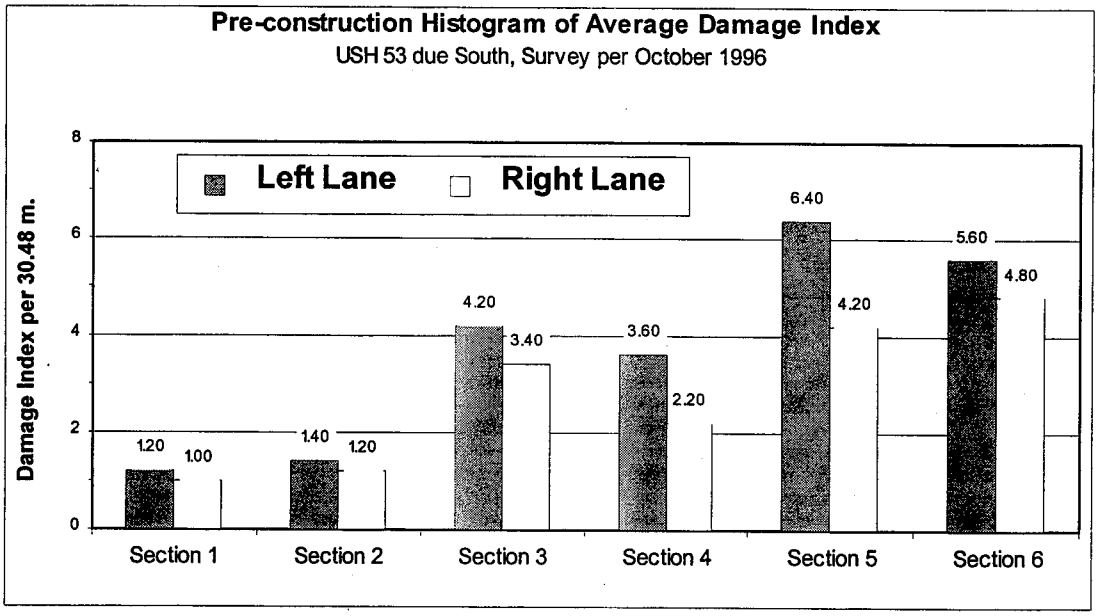

Figure 4.2 Condition of Existing Pavement Sections Prior to Construction

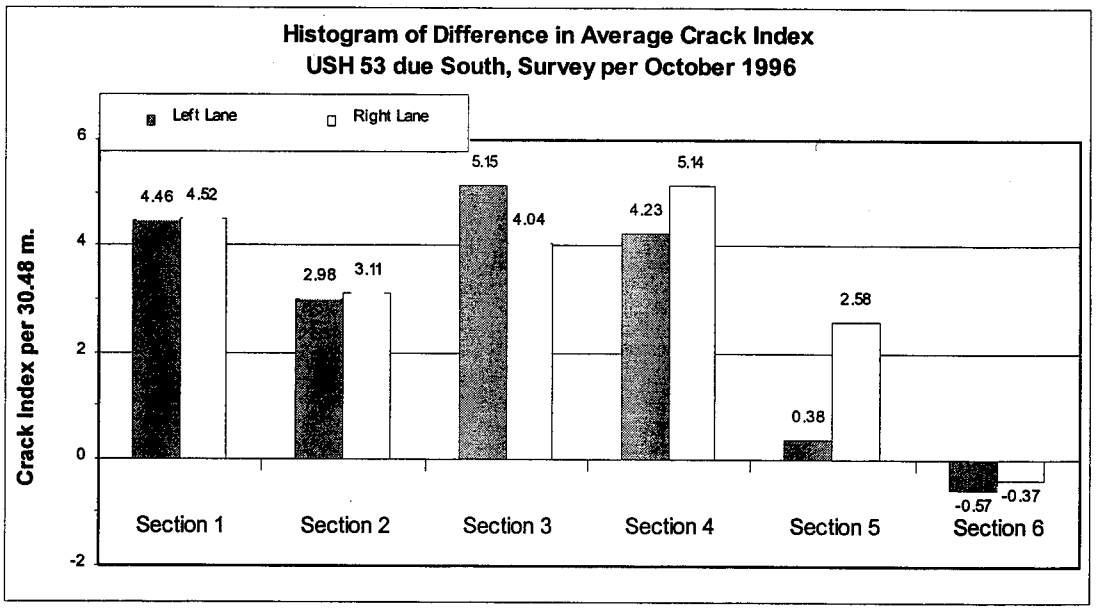

Figure 4.3 Difference in Condition of Pavement Sections as a Result of Reflective Cracking

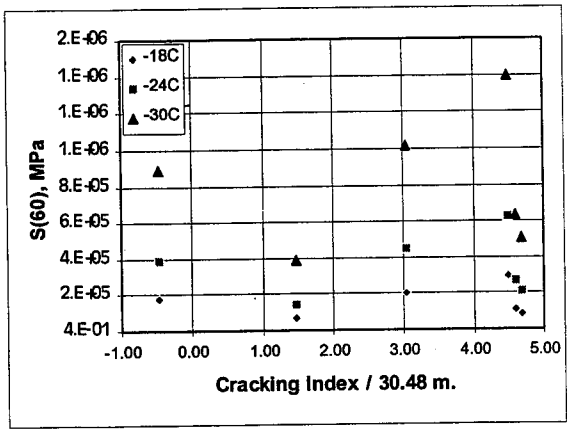

(a)

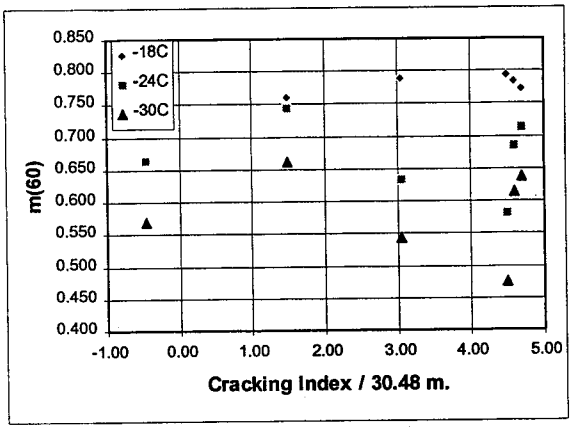

(b)

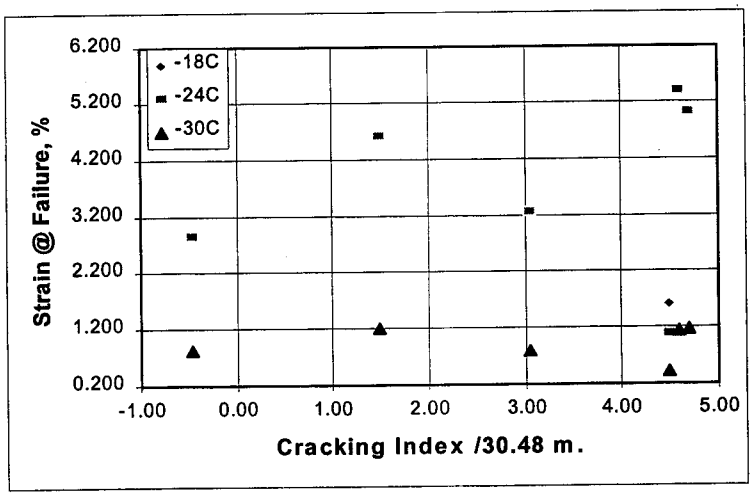

(c)

Figure 4.4 Relationship between Binder Properties and Pavement Performance

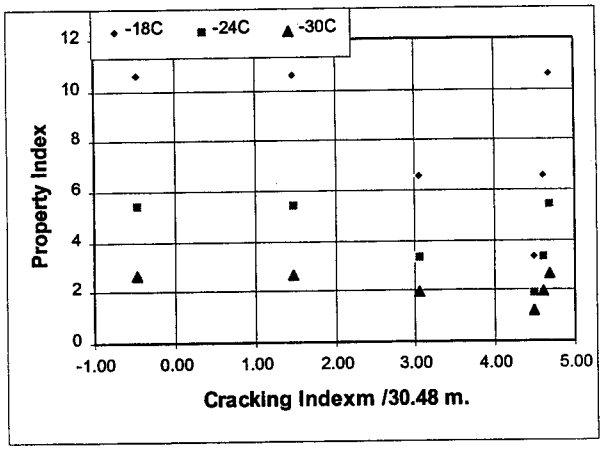

(a)

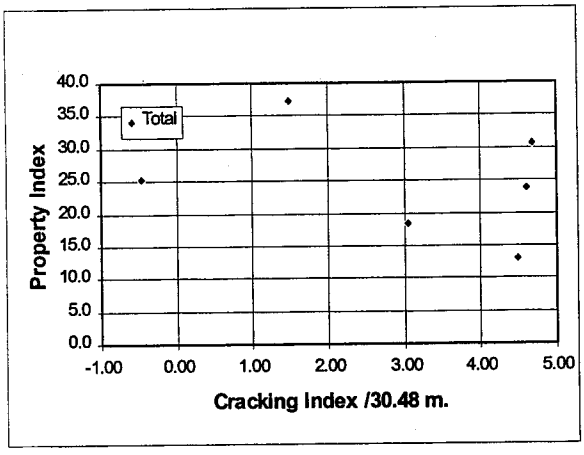

(b)

Figure 4.5 Relationship between Binder Properties Index and Pavement Performance

Figure 4.4 indicates that there is no strong correlation between the individual properties and severity of cracking irrespective of test temperatures. The Figure shows that cracking indices can be higher for lower stiffness values and /or higher m values. The lack of correlation is also observed for cracking index with the failure strain measured using the direct tension test device.

Figure 4.5 introduces the relation with the property index. As indicated before, the property index is the relative measurement of binder property to its limit in Superpave™ specification. For example, an asphalt binder with the S(60) of 250 MPa and m(60) of 0.350. Since the limits for these parameters are 300 MPa maximum for S(60) and 0.300 minimum for m(60), the property index of this binder is 2.37 calculated by adding 300/250 = 1.2 for S(60) and 0.35/0.30 = 1.17 for m(60). The higher the index, the better the asphalt is. The property index in Figure 4.5a is the total of indexes for S(60), m(60), and ε_f at each test temperature, while Figure 4.5b is the total of three properties at three temperature.

The reason for using the property index is to determine whether the properties of the binders collectively can show more significant relationship with the cracking index. The results are not very encouraging. Similar to Figure 4.4, the data in Figure 4.5 does not show strong correlations. There appears to be no relation between the quality of asphalt binder as determined by the property indices and the level of cracking observed.

It is also important to note here that Superpave™ parameters were not intended for reflective cracking. It was however expected that the binders with better low-temperature properties will show better resistance to reflective cracking since they are less stiff and more capable of stress relaxation. Also the strain at failure property index was expected to show relationship with reflective cracking since it is a failure property. It appears that the improved low-temperature properties of the modified binders did not result in better resistance to reflective cracking.

4.5 Validation of Superpave™ Binder Specification Criteria

The validation of Superpave™ binder specification limits could not be conducted because reflective cracking occurred on all test sections instead of thermal cracking. In addition Figures 4.4 and 4.5 show that there is no strong correlation observed to relate the binder properties to level of reflective cracking observed on the test sections. Superpave™ binder specification criteria were not designed to control reflective cracking and therefore it is not possible to draw any conclusions related to the limits in the Superpave™ binder specification. It is important to note however that it was expected that sections with modified binders will show better resistance to reflective cracking based on their better low-temperature properties. The sections with modified binders showed equal or more reflective cracking. This raises some questions about the value of these modified asphalts for this type of failure.

Based on information from the WisDOT, the cost of the binders were as follows;

1. Control binder: pen grade 120/150 (also PG 58-28) ; $0.115/kg
2. Modified Binder PG 58-34 grade ; $0.230/kg
3. Modified Binder PG 58-40 ; $0.260/kg

The increase in cost based on these estimates ranges between 100% and 126% compared to the control binder. The additional cost cannot be justified based on the results obtained in this study. This finding however should not be generalized for all modified binders. It is not known whether other modified binders can perform better than the binders used in this study. The criteria used in selecting the asphalts did not include resistance to reflective cracking. It was expected that because of the crack and seat treatment of the existing pavement, no reflective cracking will occur.

CHAPTER FIVE
RESEARCH FINDINGS AND RECOMMENDATIONS

5.1 RESEARCH FINDINGS

Six test sections were constructed on US Highway 53 in Trempealeau County in northwestern Wisconsin. The construction included crack and seat of the existing Portland cement concrete (PCC) pavement and overlaying with 114 mm (4.5 in) MV type asphalt concrete layer. The overlay included a binder course approximately 70 mm (3.0 in) thick and a surface course that is approximately 38mm (1.5 in) thick. The layers of the test sections were similar in all aspects except the type of asphalt cement (liquid) used in each of the two layers. Six different combinations of binder course and surface course asphalts were used to study the effect of binder grades on thermal cracking of the sections.

The asphalts used included a conventional straight run asphalt of 120-150 penetration grade that also graded as a PG 58-28. The modified asphalts included a PG 58-34 and a PG 58-40 grade. Two of the test sections were instrumented with two temperature sensors made of materials with different conductivity. In each test section, the sensors were installed at the center of one lane. Each temperature sensor allowed the measurement of temperature at four different depths. In addition to the pavement temperature sensors, a meteorological station was constructed to measure air temperature, solar radiation, wind speed and direction, and relative humidity. Data from the meteorological station and the pavement sections were collected continuously at one hour intervals for 22 months starting in December of 1994.

A comprehensive statistical analysis of the date was conducted to develop a model to predict pavement temperature as a function of depth from meteorological data. The model developed (herein termed the Wisconsin model) was compared with similar models developed by the Strategic Highway Research Program (SHRP) and more recently, by the Long Term Pavement Performance Program (LTPP). In addition to the development of pavement temperature models, the properties of the binders measured at pavement temperatures were correlated with the pavement performance determined by surface condition surveys conducted before construction and subsequently in October of 1996.

The following findings summarize the results of the different analyses of data collected in this project:

1. Using least squares statistical regression, a model was developed to predict minimum pavement surface temperatures from air temperatures:

$$T_{PAV@SURFACE(MIN)} = 0.286 + 0.695\,T_{AIR(MIN)} \quad (5.1)$$

where $T_{PAV@SURFACE(MIN)}$ = Minimum pavement temperature at surface, °C;

$T_{AIR(MIN)}$ = Minimum air temperature, °C.

The model has an R^2 value of 91.68 % and a standard error of estimate of 1.73 °C. The model shows a very good agreement with the LTPP model (equation 1.5) but does not show good agreement with the SHRP model that assumes air temperature to be equal to pavement surface temperature. The SHRP model was found too conservative in estimating the pavement surface temperature. For the Wisconsin model (Equation 5.1) it was found that including an indicator of thermal history of the pavement can significantly improve the accuracy of the prediction. The best recommended model that includes thermal history is shown in Equation 5.2. Notice that Equations 5.1 and 5.2 should be used only when the minimum air temperature is lower than -5 °C.

$$T_{PAV@SURFACE(MIN)} = -1.102 + 0.425\,T_{AIR(MIN)} + 0.362\,T_{AIR-01} \quad (5.2)$$

where $T_{PAV@SURFACE(MIN)}$ = Minimum pavement temperature at surface, °C;

T_{AIR-01} = Average air temperature one day before the day of the minimum air temperature, °C.

This model has a value of R^2 of 95.9 % and a standard error of estimate of 1.22 °C.

2. For estimation of maximum pavement design temperature, the model using only air temperature as the predictor showed a very low R^2 (25.1 %) and a very high standard error of estimate (4.4 °C). Solar radiation and thermal history had to be included in the model in order to have a better prediction. The Wisconsin recommended maximum temperature model is shown in Equation 5.3. Note that this model should be used when the pavement temperature is above 40 °C.

$$T_{PAV@20mm(MAX)} = -8.424 + 0.710\sqrt[4]{Solar_{-0} * T^2_{AIR(MAX)}} + 0.485\,T_{AIR-01} + 0.259\sqrt[4]{Solar_{-0} * MS_{-0}} \quad (5.3)$$

where $T_{PAV@SURFACE(MAX)}$ = Maximum pavement temperature at surface, °C;

$T_{AIR(MAX)}$ = Maximum air temperature, °C;

$Solar_{-0}$ = Daily total solar radiation intensity, Watt/m^2; and

MS_{-0} = Daily peak of solar radiation intensity, Watt/m^2.

This model has an R^2 value of 91.60% and a standard error of estimate of 1.87 °C. The model does not show a good agreement with LTPP (Equation 1.6) nor with the SHRP (Equations 1.2 and 1.3) high temperature models. Neither LTPP nor SHRP incorporate solar radiation, but use latitude as a substitute. Solar radiation plays an important role in determining the maximum pavement temperature and it is strongly recommended that solar radiation intensity be measured besides the air temperature.

The maximum pavement temperature at depth d can be calculated using the following equation:

$$T_{d(MAX)} = T_{PAV@SURFACE(MAX)} * \left[1 - 4.1987 \times 10^{-4}\,(d - 6.4)\right] + 1.020 \times 10^{-5}(d - 6.4)^2 \quad (5.4)$$

where $T_{d(MAX)}$ = Maximum pavement temperature at depth d, °C;

$T_{PAV@SURFACE(MAX)}$ = Maximum pavement temperature at surface, °C; and

d = Depth from surface, mm.

3. The standard deviation of the extremes daily (minimums and maximums) pavement surface temperature was found to be significantly different from the standard deviation of the daily air temperature. The standard deviation for the pavement surface is lower than air temperature at low temperatures (below approximately 10 °C) but is significantly higher at higher temperatures. The standard deviation is highly sensitive to the averaging procedure used. The standard deviation of pavement temperature based on the 7-day moving average is significantly less than the standard deviation based on the daily maximum temperature. This finding is important with regard to estimation of reliability factors in the Superpave™ binder specification system. The current specification system recommends using the standard deviation of air temperature rather than the pavement temperature. The following equations were developed to estimate standard deviation of pavement temperature from standard deviation of maximum daily air temperature. Equation 5.5 is for low temperatures and Equation 5.6 is for high temperatures.

$$STDEV_{PAV(MIN)} = 1.170 + 0.6422\, STDEV_{AIR(MIN)} \quad (5.5)$$

$$STDEV_{PAV(MAX)} = 1.694 + 1.2733\, STDEV_{AIR(MAX)} \quad (5.6)$$

As evident from the equations the daily pavement temperature standard deviations are smaller at minimum temperatures but higher for maximum temperatures. It is important to mention that these relations are based on limited data points. These equations can be used for Wisconsin and other areas that have the same pattern of solar radiation and temperature fluctuations. It is not recommended, however, that these relations be generalized for other areas.

4. Reflective cracking was observed on all six test sections. However, the severity of the cracks varied among the sections. The asphalt binders used to construct the sections were tested using Superpave™ binder testing protocols. The results of testing the asphalts, however, could not be used to fully explain the difference in reflective cracking observed on these sections. Correlation between binder properties and severity of cracking did not show

reasonable trends. The lack of correlation between asphalt binder properties and reflective cracking indicates that the modified binders used did not result in better resistance to reflective cracking.

5. Superpave™ binder specification criteria limits could not be validated because reflective cracking occurred instead of the anticipated thermal cracking. Superpave™ criteria were developed to control thermal cracking rather than reflective cracking.

6. The temperature differential between the surface layer and the bottom layer of the pavement during the time of daily maximum and minimums were found to be relatively high. The differential when the daily maximum temperatures are considered showed an average of 3.5 °C per 25.4 mm of depth.

7. The peak daily solar radiation was found to vary significantly with the month. The monthly total increases by more that 10 times between December and June. This variation has a significant impact on relation between air temperature and pavement temperature.

8. Pavement temperature was found to follow very closely the trend of air temperature. The increase and decrease rates of pavement temperature and air temperature are, however, different. During the day, the increase rate of pavement temperature is usually higher than the increase rate of air temperature due to the effect of solar radiation on the pavement surface. However, during the night, the decrease rate of pavement temperature is lower than air temperature due to the fact that the pavement retains the heat received from solar radiation during the preceding daytime. As a result, it can be commonly observed that peaks of pavement temperature are higher than the air temperature.

9. The daily minimums and maximum of pavement surface temperature are always higher than daily minimums of air temperature. The trend in differences of daily minimums cannot be attributed to a single factor (e.g., solar radiation). It appears that a combination of factors affects this difference. The daily differential in temperature between top and bottom of

pavement layer varied significantly depending on the temperature range, thermal history, and solar radiation. The current findings should stimulate discussion about the importance of variation of temperature with depth and how binders should be selected for pavements of different depths.

5.2 RECOMMENDATIONS

Based on the results of this study the following recommendations are made:

1. The models developed in this study to estimate pavement minimum and maximum temperatures (called here the Wisconsin Models) should be used to define the PG grades for Wisconsin. These models are different than the original models proposed by SHRP. The reliability factors should be based on the daily standard deviations calculated using the models developed in this study. The use of air temperature standard deviation is not realistic and is shown in this study to give an erroneous estimate of the pavement standard deviation.

2. Wisconsin DOT should continue to collect data to relate pavement temperature to air temperature. This is needed to further verify the Wisconsin models developed in this study for other regions within the State.

3. The modified binders used in this study did not result in better resistance to reflective cracking. The extra cost of these modified binders cannot be justified based on the results of this study. Modified PG graded asphalts should not be used unless a study shows that they can effectively result in less reflective cracking.

4. This project was focused more on thermal cracking rather than reflective cracking. The intention was to study the role of modified binders in reducing thermal cracking. The results indicate that what can be considered better properties for thermal cracking (e.g. lower S(60), higher m(60), and higher strain at failure) may not be necesarily better for

reflective cracking. Since reflective cracking is an important distress type in Wisconsin, a more thorough study on the possible methods to reduce or delay reflective cracking is recommended.

REFERENCES

Aldrich, H.P. (1956). "Frost Penetration Below Highway and Airport Pavements." *Bulletin 135*, HRM, National Research Council, Washington, DC.

Bahia, H.U., Anderson, D.A. (1995). "The SHRP Binder Rheological Parameters: Why Are They Required and How Do They Compare to Conventional Properties." *Preprint*, Transportation Research Board 74th Annual Meeting, Washington, DC.

Barth, E.J. (1962). Asphalt, Science and Technology, Gordon and Breach, New York, NY.

Benson, C. H. and Bosscher, P. J. (1992). "Effect of Winter Exposure on the Hydraulic Conductivity of a Test Pad." *Environmental Geotechnics Report 92-8*, Department of Civil and Environmental Engineering, University of Wisconsin at Madison.

Benson, C. H., Bosscher, P. J., Lane, D. T., and Plisca, R. J. (1994). "Monitoring System for Hydrologic Evaluation of Landfill Covers." *Geotechnical Testing Journal*, GTJODJ, Vol. 17, No. 2.

Chatterjee, S., Price, B. (1991). Regression Analysis by Example, John Wiley & Sons, Inc., New York, NY.

Draper, N.R. and Smith, H. (1981). Applied Regression Analysis, John Wiley & Sons, New York, NY.

FHWA, LTPP Division, (1994). "Specific Pavement Studies Experimental Design and Research Plan for Experiment SPS-9A." FHWA, Turner-Fairbank Highway Reaserch Center, Virginia.

Fwa, T.F., Low, B.H., and Tan, S.A. (1995). "Laboratory Determination of Thermal Properties of Asphalt Mixtures by Transient Heat Conduction Method." *Transportation Research Record 1492*, TRB, National Research Council, Washington, DC.

Kennedy, T.K., et. al. (1994). "Superior Performing Asphalt Pavements (Superpave): The Product of the SHRP Asphalt Research Program." *Strategic Highway Research Program*, National Research Council, Washington, DC.

Kreith, F. (1958). Principles of Heat Transfer, Intext Educational Publisher, New York, NY.

Lytton, R.L., et al. (1990). "An Integrated Model for the Climatic Effects on Pavements." Report No. FHWA-RD-90-033, FHWA, McLean,, VA.

Lytton, R.L., Roque, R. et. al. (1993). "Development and Validation of Performance Prediction Models and Specifications for Asphalt Binders and Paving Mixes." SHRP, National Research Council, Washington, DC.

McGennis, R. B., Shuler, S., and Bahia, H. U. (1994). "Background of Superpave Asphalt Binder Test Methods." *National Asphalt Training Center, Demonstration Project 101*, Publication No. FHWA-SA-94-069, FHWA, Lexington, KY.

Mohseni, A. (1996). "LTPP Seasonal AC Pavement Temperature Models." FHWA-LTPP Division, McLean, VA.

Rada, G.R., Elkins, G.E., Henderson, B., and Van Sambeek, R.J., Lopez, Jr., A. (1994). "LTPP Seasonal Monitoring Program: Instrumentation Installation and Data Collection Guidelines." Report No. FHWA-RD-94-110, FHWA, McLean, VA.

Rigo, J.M. (1993). "General Introduction, Main Conclusion of the 1989 Conference on Reflective Cracking in Pavements, and Future Prospect." *Proceeding of the Second International RILEM Conference, Leige University, Belgium*, Leige, Belgium.

Solaimanian, M., Bolzan, P. "Analysis of the Integrated Model of Climatic Effects on Pavements: Sensitivity Avalysis and Pavement Temperature Prediction." SHRP-A-637.

Traxler, R.N. (1961). Asphalt, Its Composition, Properties and Uses, Reinhold Publishing Corporation, New York, NY.

Waggonet, J. and O'Rouke, J. (1991). "A Computer-Assisted Automated Data Aquisition System for Remote Monitoring." *Proceedings*, Geotechnical Engineering Congress 1991, Vol. II GSP No. 27, F. McLean, D. Campbell, and D. Harris, Eds., New York, NY.